Chemical Geology 349–350 (2013) 36–53

Contents lists available at SciVerse ScienceDirect

Chemical Geology

journal homepage: www.elsevier.com/locate/chemgeo

Payenia volcanic province, southern Mendoza, Argentina: OIB mantle upwelling in a backarc environment

Nina Søager [a,*], Paul Martin Holm [a], Eduardo Jorge Llambías [b]

[a] University of Copenhagen, Department of Geosciences and Natural Resource Management, Øster Voldgade 10, DK-1350 Copenhagen, Denmark
[b] Universidad Nacional de la Plata, Facultad de Ciencias Naturales y Museo, Calle 1 Nº 644, La Plata, Argentina

ARTICLE INFO

Article history:
Received 1 August 2012
Received in revised form 6 April 2013
Accepted 7 April 2013
Available online 13 April 2013

Editor: L. Reisberg

Keywords:
Intraplate basalts
Backarc volcanism
Shallow subduction
Crustal contamination

ABSTRACT

The Pleistocene to Holocene Payenia volcanic province is a backarc region of 60,000 km^2 in Mendoza, Argentina, which is dominated by transitional to alkaline basalts and trachybasalts. We present major and trace element compositions of 139 rocks from this area of which the majority are basaltic rocks with 4 to 12 wt.% MgO and 44 to 50 wt.% SiO_2. The southern Payenia province is dominated by intraplate basalts and the trace element patterns of the Río Colorado and Payún Matrú lavas suggest little or no influence from subducted slab components. The mantle source of these rocks is similar to some EM-1 ocean island basalts. In contrast, the magmas from the northern Payenia province and the Andean retroarc occurrences have received an important input from the subducting slab and their trace element patterns are transitional between intraplate and arc rocks. These magmas are mainly derived from another asthenospheric mantle source which may be similar to normal MORB mantle. The Nevado and Northern Segment basalts have presumably been formed above a shallowly subducting slab and the progression of volcanism from south to north and northwest along the San Rafael block likely marks the downwarping of the slab and the end of the shallow subduction period. The downwarping slab may have generated an enhanced mantle upwelling of both the intraplate and the MORB-like mantle sources.

In samples from almost all parts of the Payenia province and in particular many Nevado, Llancanelo and older Payún Matrú basalts, trace element variations suggest a significant contribution from lower crustal melts, possibly up to 70% in the most extreme cases. The contaminating lower crustal rocks must have been depleted mafic rocks with a plagioclase component. The extensive melting of lower crust is probably related to the low thickness of the lithospheric mantle and preheating of the lower crust by earlier Mio-Pliocene volcanism. Rare earth element modelling of mantle melting calls for enriched source compositions and a beginning of melting within the garnet stability field for all Payenia basalts. The Río Colorado and Payún Matrú basalts indicate high solidus pressures around 3–3.1 GPa which requires either a thermal or compositional mantle anomaly. The model suggests a thinner lithosphere in the western Payenia region compared to the eastern.

1. Introduction

Extensive alkaline basaltic volcanism has prevailed in the Andean backarc region, the Payenia volcanic province, during the Pleistocene and Holocene after a period of sub-alkaline volcanism in the Miocene (e.g. Kay and Copeland, 2006; Kay et al., 2006a, 2006b; Litvak et al., 2008). The cause for this alkaline volcanism up to 500 km away from the trench has long been a matter of speculation (e.g. Stern et al., 1990; Kay et al., 2004). Alkaline OIB-type intraplate volcanism occurs throughout Patagonia alongside basaltic backarc lavas affected by subduction zone fluids, and the Payenia province is the northernmost of these volcanic provinces. The southern Patagonian magmatic provinces were proposed to have formed above transient thermal anomalies and slab-windows caused by ridge subductions (summary and references in Kay et al., 2004) whereas the Payenia volcanism has been explained as a consequence of influx of hot asthenospheric mantle into the mantle wedge after a period of shallow subduction during middle to late Miocene times. This influx should then have caused the already hydrated upper mantle to melt (the so-called "wetspot melting") (Kay, 2001; Kay et al., 2004, 2006a; Kay and Jones, 2011). Bermudez et al. (1993) and Bertotto et al. (2009) suggested that the arc-signature in the erupted lavas has decreased with time supporting the theory of wetspot melting but Bermudez et al. (1993) also concluded that the arc-signature of the lavas is independent of the distance from the trench. Furthermore, Kay (2001), Germa et al. (2010) and Hernando et al. (2012) proposed a plume-like mantle source for the southern Payenia rocks with minimal influence from slab fluids. This suggests that the southern Payenia basalts have been

* Corresponding author. Tel.: +45 35322467; fax: +45 35322501.
E-mail address: ns@geo.ku.dk (N. Søager).

0009-2541/$ – see front matter © 2013 Elsevier B.V. All rights reserved.
http://dx.doi.org/10.1016/j.chemgeo.2013.04.007

generated by a different mechanism and therefore Kay et al. (2004) and Kay et al. (2006a) proposed that the Patagonian mantle is hotter than normal mantle and that the southern Payenia volcanism was triggered by tectonic perturbations of this hot mantle.

On the basis of our new major and high precision trace element analyses of 139 samples from the backarc province, we discuss the geochemical variations in relation to age and geographical position. The assessment of the role of the subducting Nazca plate and the asthenospheric and lithospheric mantle sources in the genesis of the volcanism suggests that the backarc volcanism in the northern Payenia and the intraplate volcanism in the southern Payenia region are fed from two distinct asthenospheric mantle sources. Lower crustal contamination is interpreted to play an important role in the area and possibly amounts to up to 70% in some lavas. Furthermore, we present a model for the mantle melting systematics based on rare earth element variations and a model for the fractional crystallisation of the most primitive Payún Matrú complex basalts.

2. Geological background

The studied area stretches from the upper Pleistocene Cerro Diamante volcano in the north at 34° 38′S to the cones and flows around Río Colorado just north of the town Rincón de los Sauces ~37° 24′S. The westernmost volcano represented in this study is the Volcán El Gaucho at 70° 02′W in the Andean Principal Cordillera (340 km east of the oceanic trench) whereas the easternmost lava was collected at ~67° 58′W (500 km from the trench) (Fig. 1).

The area is an extensive backarc volcanic field situated at the same latitudes as the Andes Transitional Southern Volcanic Zone (TSVZ). The Nazca plate is currently subducted under South America at a speed of ~6.6 cm/a with an azimuth of 79.5° (Kendrick et al., 2003), and the slab dip is ~30° with recorded seismicity from the slab down to 200 km depth (Cahill and Isacks, 1992). The volcanic backarc province is bounded to the south by the NW-trending Tromen–Domuyo belt of volcanism (TDB in Fig. 1) (Llambías et al., 2010) associated with the Cortaderas lineament, which is a basement discontinuity extending into the high Andes (Ramos and Kay, 2006, and references herein) (Fig. 1).

The main structural elements in the area are the Principal Cordillera, the central depression (CD in Fig. 1) and the San Rafael block (SRB) (Ramos and Kay, 2006; Llambías et al., 2010). The eastern part of the principal Cordillera is dominated by the Malargüe fold and thrust belt (MFTB), that was formed by thick-skinned stacking of Mesozoic sedimentary rocks and the Permo-Triassic basaltic to rhyolitic volcanic and plutonic rocks from the Choiyoi group (e.g. Llambías et al., 1993). The deformation occurred between 15 Ma and Lower Pleistocene times but the rate of deformation strongly decreased after 8 Ma (e.g. Giambiagi et al., 2008; Turienzo, 2010). In the central depression just east of the principal Cordillera, around 1000 m of syn-orogenic continental Cenozoic deposits have been accumulated (Yrigoyen, 1993; Manacorda et al., 2002; Ostera and Dapeña, 2003). The depression runs approximately N–S in between the western thrust front in the west and the N–S trending Llancanelo fault in the east down to Payún Matrú, and its sediments overlie the Mesozoic sediments of the Neuquén basin, which also form substrate to the southern part of the volcanic province. The depression fades out south of Payún Matrú. The San Rafael basement block (SRB) was uplifted by compressional tectonics in the late Miocene. It is bounded by the Llancanelo fault in the west and the eastern thrust front, i.e. the Cerro Negro and Las Malvinas fault systems, in the east (Fig. 1). The uplifted block is segmented into smaller blocks and cut by NW–SE trending faults formed during the lower Pleistocene (Folguera et al., 2009).

The compressional tectonics that lead to the formation of the Malargüe fold and thrust belt, the central depression and the uplift of the San Rafael block were induced by the shallow subduction during middle and late Miocene and Pliocene times (Kay, 2002; Kay et al., 2004). This is evidenced by the occurrence of subduction related volcanic rocks up to 500 km east of the present trench, among others the Cerro Nevado and Cerro Chachahuén (Kay and Copeland, 2006; Kay et al., 2006b; Litvak et al., 2008). According to Folguera et al. (2009) there was a relaxation of the crust in both the arc and backarc due to extension of the crust after the period of shallow subduction and this caused normal faulting in the San Rafael block. However, the observed Pleistocene to recent movements in the eastern San Rafael block faults were reverse (Costa et al., 2004, 2006; Folguera et al., 2009) and the Pleistocene structural history of the San Rafael block is still unclear. The present stress field is weakly compressional, as displayed by maximum horizontal stress orientations from borehole breakout analyses (Guzmán et al., 2007) and GPS measurements (Klotz et al., 2001; Wang et al., 2007). Also the E–W trending eruptive fissures characteristic of the late Pleistocene to Holocene volcanism in e.g. the Llancanelo and Payún Matrú regions could have been formed by compressive forces, instigated by the plate boundary and topographic load forces acting perpendicular to the Andes (Guzmán et al., 2007; Mazzarini et al., 2008).

3. Age and geology of the volcanic fields of Payenia

The Payenia back-arc field was previously divided into two volcanic fields by Bermudez et al. (1993), but to investigate our dataset in more detail, the volcanic fields are further subdivided according to geographical position, age and geochemical characteristics using the groups defined by Gudnason et al. (2012). These are largely the same as used by Ramos and Folguera (2011). The map in Fig. 1 shows the sample locations and volcanic fields.

3.1. Northern Payenia

In the Nevado volcanic field, NW-trending normal faults and the N–S trending thrust faults exerted a major control on the position of the volcanoes (Mazzarini et al., 2008; Folguera et al., 2009). Apart from the large stratovolcano Cerro Nevado, the Nevado area is characterised by small to medium-sized often polygenetic volcanoes such as Ponon Trehué, along with monogenetic cones and lava flows. Folguera et al. (2009) and Gudnason et al. (2012) showed that volcanism progressed gradually northwards from the southern Nevado volcanic field in the late Pliocene to the northern Nevado volcanic field ~800 ka ago. Thereafter, volcanism moved NW to the Northern Segment in the late Pleistocene, where the large composite volcano Cerro Diamante displayed some of the latest activity with ages down to 54 ± 12 ka (2σ) (Folguera et al., 2009).

In the Llancanelo volcanic field, most of the volcanoes are positioned along relatively short ENE–WSW trending fractures (Mazzarini et al., 2008; Risso et al., 2008). The youngest volcanic products with ages ~50–100 ka (Españon, 2010; Gudnason et al., 2012), include small monogenetic volcanoes and scoria cones with associated lava flows but also hydromagmatic products (Risso et al., 2008). The cones are positioned on basalt plateaus of which one of the oldest lavas sampled yielded and Ar/Ar age of 1.1 ± 0.2 (2σ) Ma (Dyhr et al., in prep. b).

3.2. Southern Payenia

In the Payún Matrú volcanic field the most recent volcanic activity of the Payenia province is found (Bermudez et al., 1993; Germa et al., 2010). Payún Matrú (PM in Fig. 1) is a large basaltic shield volcano topped by a trachytic strato-cone which was subject to a caldera collapse ~168 ka ago (Germa et al., 2010). It is positioned above the E–W trending, 70 km long Carbonilla fault (CF) (Llambías, 1966). The Pampas Negras (PN) and Los Volcanes (LV) basalts were erupted from the western sector of the Carbonilla fault. Pampas Negras is dominated by scoria cones and lava flows while Los Volcanes is a basaltic flow field

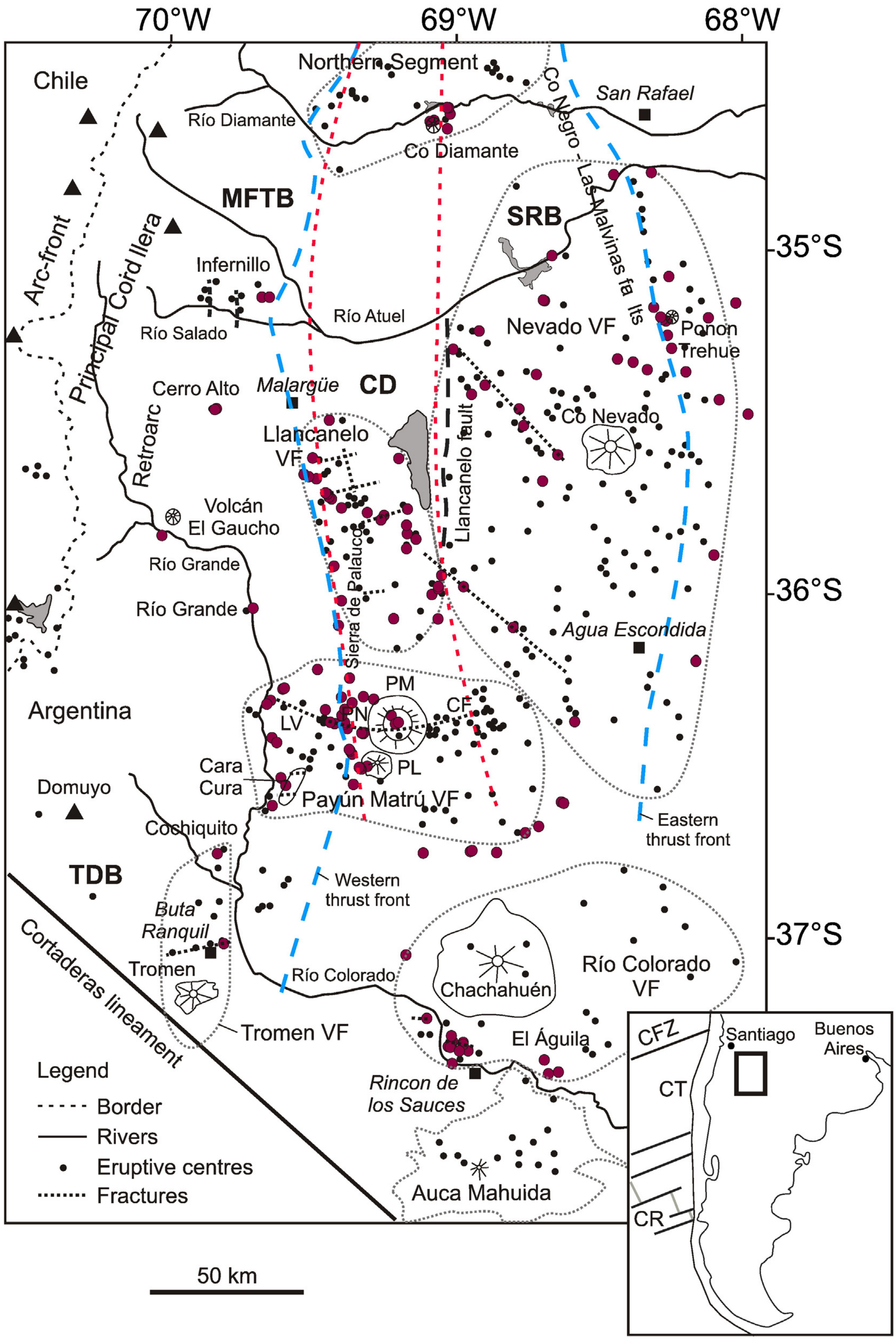

Fig. 1. Map of the Payenia province with the volcanic fields outlined in grey. Sample locations are indicated with red dots. The black dots mark cones and eruption centres and the black triangles are the volcanoes of the present Andean arc. The major volcanoes are shown. The structural elements the San Rafael block (SRB), the central depression (CD) (outlined by the orange dashed lines) and the Malargüe fold and thrust belt (MFTB) all run approximately north–south. The Tromen–Domuyo belt (TDB) of volcanism is largely coincident with the Cortaderas lineament. Abbreviations: VF: volcanic field, LV: Los Volcanes, PN: Pampas Negras, PM: Payún Matrú volcano, PL: Payún Liso volcano, and CF: Carbonilla fault. The shown volcanoes and sample localities are all upper Pliocene to Holocene of age except the Miocene Chachahuén volcanic complex. Blue dashed lines outline the major thrust fronts. The western thrust front forms the eastern boundary of the MFTB. The inset shows the location of the studied area in southern South America. CR: Chile Ridge, CFZ: Challenger fracture zone, and CT: Chile trench.

with numerous large flows and fewer cones. The eastern extension of the Carbonilla fault is also marked by numerous cones and was the source of the large Pleistocene flood basalts, here called Payún Matrú east basalts, which were described by Mazzarini et al. (2008) and Pasquaré et al. (2005, 2008). Detailed maps of the Payún Matrú complex are found in Llambías (1966), Hernando et al. (2012) and Mazzarini et al. (2008). The Payún Matrú complex including the Payún Liso stratocone (PL) was presumably formed primarily from ~320 ka up to historical times (González Díaz, 1972; Germa et al., 2010; Gudnason et al., 2012). However, the Payún Matrú east basalts have been formed over a longer period of time since the Pliocene according to a new Ar/Ar age of 2.94 ± 0.11 Ma (Dyhr et al., in prep. b) and K/Ar ages from Núñez (1976) and Melchor and Casadío (1999).

The Cara Cura eruption centres just south of Los Volcanes include three larger cones with associated lava flows and five smaller scoria cones which are all positioned along two fractures in the Sierra de Cara Cura (Fig. 1). In the Río Grande valley just east of the cones are at least 5 larger, older lava flows (probably of upper Pleistocene age) extending >20 km along the eastern side of Río Grande down to Cochiquito volcano. These flows are apparently derived from the Cara Cura eruption centres. Sample 126239 is from the northernmost of these flows.

The Río Colorado volcanic field includes the late Pliocene to Pleistocene volcanic activity occurring in and around the Chachahuén volcanic complex and Colorado river (described by Bertotto et al. (2000, 2003, 2006, 2009), Kay (2001) and Kay et al. (2004)). In this paper, only data from the Colorado river valley are presented. The easternmost group of cones is oldest with an age of 1.5 Ma ± 0.13 (2σ) for Cerro El Águila (Gudnason et al., 2012). Further upstream, the younger volcanic complexes were mainly erupted between 1.23 Ma ± 0.34 (2σ) (Kay et al., 2006b) and 0.34 Ma ± 0.13 (2σ) (Gudnason et al., 2012).

The Tromen volcanic field is composed of numerous monogenetic cones, andesitic volcanoes and rhyolitic domes of upper Pliocene to Holocene age (e.g. Kay et al., 2006a; Galland et al., 2007; Folguera et al., 2008). The three samples from the Tromen volcanic field are taken in the north-eastern part of the basaltic cone field just north of Buta Ranquil and from the Cochiquito cone.

3.3. Retroarc

The retroarc group includes the eruption centres within the Andean foothills west of the central depression. In this group are the cones by the Río Grande which have been dated by Ar/Ar to 0.72 Ma ± 0.2 (2σ) (Dyhr et al., in prep. a) and the Volcán El Gaucho volcano on the northern side of the Río Grande dated to 1.2 Ma ± 0.4 (2σ) (Gudnason et al., 2012). Cerro Alto is a small lava capped mountain top 25 km west of Malargüe. Judging from appearance, Cerro Alto is somewhat younger than the Volcán El Gaucho. The northernmost occurrence in the retroarc group is the Infernillo lavas by the Río Salado. This paper includes two samples from an eroded cone on the foreland plain around 10 km east of the main Infernillo eruption centres.

4. Petrography of the sampled rocks

Basalts from the Payenia volcanic province are generally dominated by olivine and plagioclase phenocrysts as also described by Bermudez et al. (1993). Most samples from the Nevado group exclusively contain olivine phenocrysts whereas the majority of the Llancanelo, Payún Matrú and Río Colorado basalts have olivine and plagioclase phenocrysts and some of them also clinopyroxene and/or oxide minerals. As described in detail by Hernando et al. (2012) for the Payún Matrú complex rocks, evidence for mineral disequilibrium, such as embayed olivines and sieved plagioclases, and signs of magma mingling are commonly seen in samples from the entire Payenia province. In the Los Volcanes and Pampas Negras basalts often two generations of phenocrysts are present: one has large partly resorbed and often zoned grains. Plagioclases from this generation sometimes have euhedral, zoned outer rims. The other generation of phenocrysts is smaller and sub- to euhedral. Amphibole phenocrysts are only found in three samples: one from the Cerro Alto cone in the retroarc group, one from Cerro Diamante in the Northern Segment and one from the caldera rim of the Payún Matrú volcano.

5. Analytical methods

Jaw crushed samples were powdered in an agate swing mill and major elements were analysed either at the Acme Analytical Laboratories Ltd, Canada (Acme Labs; Code 4A) or at the Geological Survey of Denmark and Greenland (GEUS). At Acme, fused glass discs were analysed by ICP-AES. Volatile contents were estimated by weight loss on ignition at 1000 °C. The reproducibility of the ICP-AES analysis has been estimated from replicate analyses of the basaltic DISKO-1 standard of the Geological Survey of Denmark and Greenland (n = 9) and an andesitic in-house standard used by Acme Labs (n = 48). The precision (2σ) is better than ±3% for most elements except for MnO (4.9 and 1.7%, DISKO-1 and in-house standard respectively), K_2O (4.6 and 0.8%) and P_2O_5 (10.4 and 4.5%). At GEUS, major elements were analysed by XRF on glass discs according to the method of Kystol and Larsen (1999). Volatile contents were estimated by weight loss on ignition and Na was analysed by flame photometry.

For trace element analysis, 0.1 g of rock powder was digested in $HF + HNO_3$. After evaporation, the samples were treated twice with concentrated HNO_3 to remove residual fluorides, dried down and thereafter dissolved in $HNO_3 + H_2O$. The samples were analysed at GEUS on a PerkinElmer 6100 DRC Quadrupole ICP-MS. Calibration was performed using international standards under the same conditions as the samples. Reproducibility has been evaluated from analysis of two international and one in-house standard (BCR-2, BHVO-2, DISKO-1, n = 18 for all three) run as unknown along with the samples and is between 2 and 8 rel.% (2σ) for most elements (see Electronic Appendix B). Selected sample results are listed in Table 1 and the full dataset is given in Electronic Appendix A.

A subset of twelve samples from the Nevado volcanic field was analysed for Nd and Sr isotopes. For this, 600 mg of hand-picked rock chips was leached for 1 h in 6 N HCl at 120 °C and the residue digested in $HF + HNO_3$. The samples were loaded onto cation exchange columns and Sr was extracted in 2 M HCl. Subsequently, the REEs were collected in 6 M HCl. Nd was separated from the REE fraction with Eichrom LN resin in 0.3 M HCl. Analyses were run in static (Sr) and dynamic (Nd) mode on a VG 54-30 MC-TIMS in the Department of Geosciences and Natural Resource Management, University of Copenhagen. The isotope results were monitored by the international standard NBS987 for Sr giving $^{87}Sr/^{86}Sr = 0.710241 \pm 0.000019$ (2σ, n = 54) and JNdi for Nd giving $^{143}Nd/^{144}Nd = 0.512096 \pm 0.000016$ (2σ, n = 52). Total procedural blanks were below 600 pg for Sr and 20 pg for Nd. See data in Table 2.

6. Results

6.1. Major elements

In the TAS-diagram (Le Maître et al., 2002) the majority of samples are classified as transitional to mildly alkaline basalts or trachybasalts (Fig. 2) and have 0–10% nepheline in the CIPW-norm assuming $Fe_2O_3/FeO = 0.3$ for basalts and trachybasalts, 0.4 for trachyandesites and 0.5 for trachytes (Middlemost, 1989). However, a few samples from each major group are sub-alkaline. The retroarc lava from the Río Grande valley is a subalkaline basaltic andesite while the two samples from Volcan El Gaucho are subalkaline trachydacites all plotting along with the Andes TSVZ rocks in Figs. 2 and 3. The other

Table 1
Major and trace element concentrations in selected Payenia rocks.

	Southern Payenia						Northern Payenia			Retroarc
Sample	123936	123944	126255	126239	126175	126174	123962	126151	126092	123915
Group	PM	PM	PM	PM	RC	RC	Nevado	Nevado	Co Dia.	Río Gr.
Major elements in wt.%										
SiO_2	46.97	47.98	45.52	47.82	46.49	46.76	49.20	46.94	46.98	52.26
TiO_2	2.02	2.31	1.86	1.35	1.63	1.52	1.01	2.45	1.53	1.12
Al_2O_3	16.25	14.77	17.16	17.26	13.72	14.91	15.17	16.42	14.79	17.16
Fe_2O_3	11.45	12.21	10.47	11.17	11.20	11.30	8.77	11.45	11.18	9.05
MnO	0.158	0.147	0.150	0.170	0.150	0.170	0.152	0.160	0.170	0.135
MgO	8.19	8.07	6.27	7.63	13.00	9.48	8.22	5.96	9.53	6.60
CaO	10.09	8.35	11.65	10.61	7.20	9.87	9.63	9.11	9.67	8.36
Na_2O	3.46	3.87	3.26	3.22	3.63	2.81	3.55	4.02	3.13	3.68
K_2O	1.22	1.48	0.97	0.41	1.78	1.12	1.43	1.63	1.10	1.06
P_2O_5	0.390	0.565	0.400	0.180	0.460	0.570	0.399	0.640	0.380	0.348
LOI	0.00	0.00	1.90	0.00	0.20	1.00	1.50	0.90	1.10	0.00
Total	99.70	99.47	99.68	99.76	99.58	99.59	99.03	99.69	99.56	99.52
Trace elements in ppm										
Sc	29.1	19.7	24.4	32.0	17.2	26.0	18.5	20.3	25.3	21.3
Ti (wt.%)	1.21	1.40	1.09	0.81	0.92	0.89	0.55	1.39	0.88	0.69
V	260	221	212	202	148	229	155	183	205	190
Cr	234	334	117	154	484	324	321	89	346	194
Mn	0.127	0.123	0.118	0.137	0.121	0.135	0.114	0.123	0.123	0.097
Co	46.0	52.2	38.3	44.8	60.0	45.1	36.8	39.7	45.2	35.3
Ni	114	190	57	95	428	199	201	57	181	89
Cu	53	54	46	61	53	48	43	48	47	39
Zn	80	116	81	72	85	87	62	100	80	61
Ga	20.1	22.1	20.4	18.4	17.9	20.3	19.3	22.0	19.0	19.6
Rb	20.8	15.6	12.6	5.3	36.0	27.1	34.3	19.0	25.4	19.0
Sr	690	880	742	401	672	974	1087	883	591	792
Y	23.3	20.3	24.1	25.1	18.7	23.0	20.4	24.6	22.9	18.4
Zr	151	185	161	108	170	120	148	183	118	141
Nb	18.6	35.5	15.6	4.8	31.7	14.2	13.7	35.3	11.5	8.0
Cs	0.71	0.25	0.42	0.12	1.02	0.81	0.83	0.31	1.00	0.54
Ba	298	307	306	165	464	608	792	370	431	470
La	16.89	23.11	15.70	8.03	23.14	24.80	30.34	26.05	18.66	22.21
Ce	38.26	47.95	35.41	19.58	45.17	49.45	57.35	53.71	39.46	46.03
Pr	4.98	6.39	4.61	2.79	5.45	6.29	6.77	6.78	5.20	5.96
Nd	22.20	27.85	20.89	13.41	22.28	26.57	26.41	28.80	22.77	24.26
Sm	5.27	6.19	4.73	3.48	4.77	5.67	5.26	6.29	5.11	4.78
Eu	1.77	2.06	1.70	1.27	1.58	1.79	1.61	2.17	1.57	1.46
Gd	5.29	5.94	5.08	4.12	4.73	5.48	5.15	6.34	5.09	4.43
Tb	0.79	0.85	0.78	0.69	0.68	0.78	0.73	0.89	0.76	0.61
Dy	4.39	4.27	4.32	4.21	3.68	4.38	3.84	4.86	4.33	3.52
Ho	0.83	0.74	0.83	0.89	0.67	0.78	0.69	0.88	0.83	0.66
Er	2.19	1.81	2.27	2.52	1.74	2.08	1.87	2.23	2.22	1.81
Tm	0.32	0.24	0.33	0.37	0.22	0.28	0.25	0.30	0.31	0.25
Yb	1.93	1.36	1.93	2.35	1.42	1.86	1.65	1.84	1.92	1.59
Lu	0.273	0.198	0.291	0.378	0.205	0.283	0.235	0.258	0.296	0.246
Hf	3.50	4.09	3.44	2.61	3.59	2.97	3.46	4.05	3.04	3.30
Ta	1.10	2.00	0.86	0.29	1.82	0.70	0.79	1.99	0.64	0.46
Pb	2.89	2.04	2.27	1.56	3.05	8.76	11.15	2.10	5.24	5.98
Th	2.07	2.09	1.20	0.62	3.26	5.29	7.57	2.17	3.47	4.23
U	0.63	0.66	0.53	0.16	0.93	1.47	1.89	0.62	0.97	0.90

Major elements are reported on a volatile free basis. PM is Payún Matrú volcanic field, RC is Río Colorado volcanic field, and Río Gr. is Río Grande.

retroarc lavas from the Infernillo region and Cerro Alto are alkali basalts and their major element compositions are more similar to the Nevado and Cerro Diamante lavas. The Payun Liso lavas are slightly more alkaline than the Payún Matrú lavas and form a continuation of the alkaline Río Colorado trend in Fig. 2.

Samples from the Nevado and Llancanelo groups come from many different, small eruptive centres and very few, if any, are related by fractional crystallisation. They are all basalts with relatively high MgO between 4.9 and 11.2 wt.% (Fig. 3), but many basalts from the Nevado group are more MgO rich and SiO_2 poor than the Llancanelo basalts as also noted by Bermudez et al. (1993). The Nevado and Llancanelo basalts generally have higher TiO_2 than the arc-rocks but sample 123962 is arc-like and has very low TiO_2 whereas sample 126151 resembles the Río Colorado basalts with high TiO_2 (2.46 wt.%).

Within the Payún Matrú volcanic field there is a difference in geochemistry between the sub-groups (Fig. 4). The basalts from Los Volcanes and Pampas Negras (grouped together as Payún Matrú basalts in Fig. 4) and Payún Matrú east and the Payún Matrú caldera and Payun Liso samples all together form a broad trend apparently controlled by fractional crystallisation as described by Hernando et al. (2012). The degree of fractionation increases from Los Volcanes, with an average of 7.14 wt.% MgO, over Pampas Negras, with an average of 6.32 wt.% MgO, to Payún Matrú caldera and Payun Liso with MgO < 3.6 wt.%. The Payún Matrú caldera and Payun Liso lavas form two distinct trends. The Payun Liso trend has higher MnO, TiO_2 and P_2O_5 but lower Al_2O_3 at a given MgO content and as in Fig. 2 form a continuation of the Río Colorado trends.

The Río Colorado lavas span a large range in MgO contents from 13 to 4 wt.% (Fig. 4). Despite the considerable variations in major

Table 2
Sr and Nd-isotopic composition of selected Nevado basalts.

Sample no.	$^{87}Sr/^{86}Sr$	2σ	$^{143}Nd/^{144}Nd$	2σ
123954	0.704027	8	0.512759	7
Duplicate	0.704034	8		
126182	0.703909	10	0.512797	31
Duplicate	0.704006	6		
123956	0.703875	10	0.512811	7
126208	0.703948	8	0.512816	9
126221	0.703911	8	0.512809	7
123940	0.703842	8	0.512824	9
126215	0.703865	10	0.512820	6
123963	0.704285	6	0.512693	18
126189	0.703937	8	0.512758	22
126163	0.704042	15		
126162	0.704126	8	0.512710	17
126187	0.704082	10	0.512782	9

2σ is given as the double standard error of the mean on the last stated digit. The duplicates are made on a second dissolution of the samples.

element contents, the Río Colorado samples have distinctly lower Al_2O_3 and higher P_2O_5 than the Payún Matrú basalts and many also have higher TiO_2, Na_2O and K_2O. The basalts from the Tromen volcanic field have major element compositions similar to the other southern Payenia basalts but have TiO_2 and FeO^T in the low end of the observed range.

The losses on ignition of the samples reach up to 2.8 wt.% but 83% of the samples have less than 1.5 wt.% and 40% have 0–0.2% volatiles. This agrees well with the generally low degree of alteration of the samples. Nevertheless, some samples contain secondary minerals such as calcite and zeolites, in particular the older samples from the Nevado, Llancanelo and Río Colorado groups.

6.2. Trace elements

Representative rare earth element (REE) patterns of basaltic samples from the various groups are rather similar with only slightly fractionated heavy REEs and gently sloped middle and light REEs (Fig. 5). The Nevado and retroarc basalts are among the most REE-enriched while the Río Colorado and Nevado lavas have the most fractionated heavy REE patterns and have higher $(Tb/Yb)_N$ (1.70–2.32) than the Payún Matrú and Llancanelo lavas (1.54–1.98).

In plots of Mg# vs. Sr, Nb and Ni (Fig. 6) the Payún Matrú basalts form trends of increasing Sr and Nb and decreasing Ni which may have been caused by fractional crystallisation of olivine and clinopyroxene. In contrast, the Nevado, Cerro Diamante and Llancanelo basalts form trends oblique to what is expected from fractional crystallisation and in particular the Nevado and Cerro Diamante samples are very primitive with high Ni and Mg#. The Río Colorado basalts are more heterogeneous but they generally have higher Nb-contents than other Payenia rocks. The Río Colorado and some Payún Matrú east basalts (here included in the Payún Matrú group) have higher Ni (Fig. 6c) and lower Sc and V (not shown) for a given Mg# than other Payenia basalts. The trace element patterns of the basalts vary between the volcanic fields and span from arc-like compositions in the retroarc lavas with high positive Pb and Sr anomalies and negative Nb–Ta and Ti anomalies, over backarc compositions in the northern Payenia basalts to intraplate compositions in the southern Payenia lavas (Fig. 7). The samples from the Llancanelo volcanic field have trace element compositions intermediate between the rocks from the northern and southern Payenia respectively. The samples that are most similar to ocean island basalts (OIB) are the Río Colorado basalts (Fig. 7a) which have low Ba/Nb, La/Nb and Zr/Nb (down to 9.3, 0.66 and 4.8, respectively) and high U/Pb, Ce/Pb, and Nb/U (up to 0.39, 29.2 and 60, respectively) (Fig. 8) reflecting the relatively high Nb and Ta concentrations and often negative Pb anomalies. A prominent feature of the Río Colorado trace element patterns is the positive Ba, K, Sr and P anomalies which are also found in the Payún Matrú and Llancanelo rocks. These features are characteristic of EM-1 ocean island basalts (Zindler and Hart, 1986) such as the Gough Island basalts (Fig. 7a), and they are also found in many Patagonian basalts, e.g. the Laguna Blanca and Somuncura basalts (Kay et al., 2004, 2007; Varekamp et al., 2010). Positive Sr and P anomalies are also seen in the Nevado, Cerro Diamante and retroarc basalts.

There are three noteworthy exceptions from the overall grouping of the dataset: sample 126151 from a presumably early Pleistocene lava collected north of Ponon Trehué in the Nevado volcanic field and sample 123944 from a large flow on the eastern flank of Payún Matrú. These samples have a geochemistry similar to the most OIB-like Río Colorado lavas with high Nb/U, Ce/Pb and U/Pb and low La/Nb and Ba/Nb as well as high TiO_2 contents and low Al_2O_3. Finally,

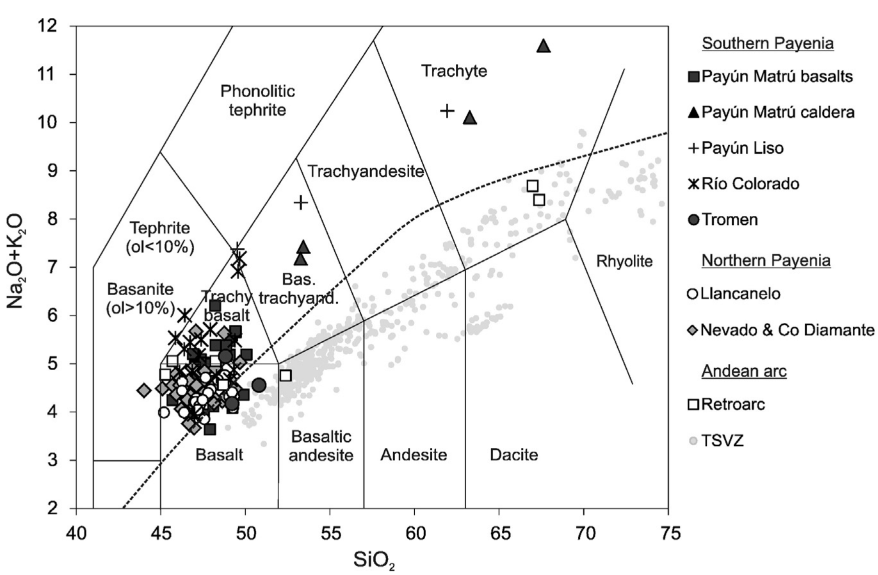

Fig. 2. Total alkalis vs. silica (TAS) diagram after Le Maître et al. (2002). The majority of the backarc samples plot as alkali basalts and trachybasalts while some of the Andes retroarc data are sub-alkaline. The dotted line separating the subalkaline from alkaline is after Irvine and Barager (1971). The Andes TSVZ (transitional southern volcanic zone) data are from a compilation of Andes data by http://georoc.mpch-mainz.gwdg.de and from Varekamp et al. (2006) and Holm et al. (in prep.)

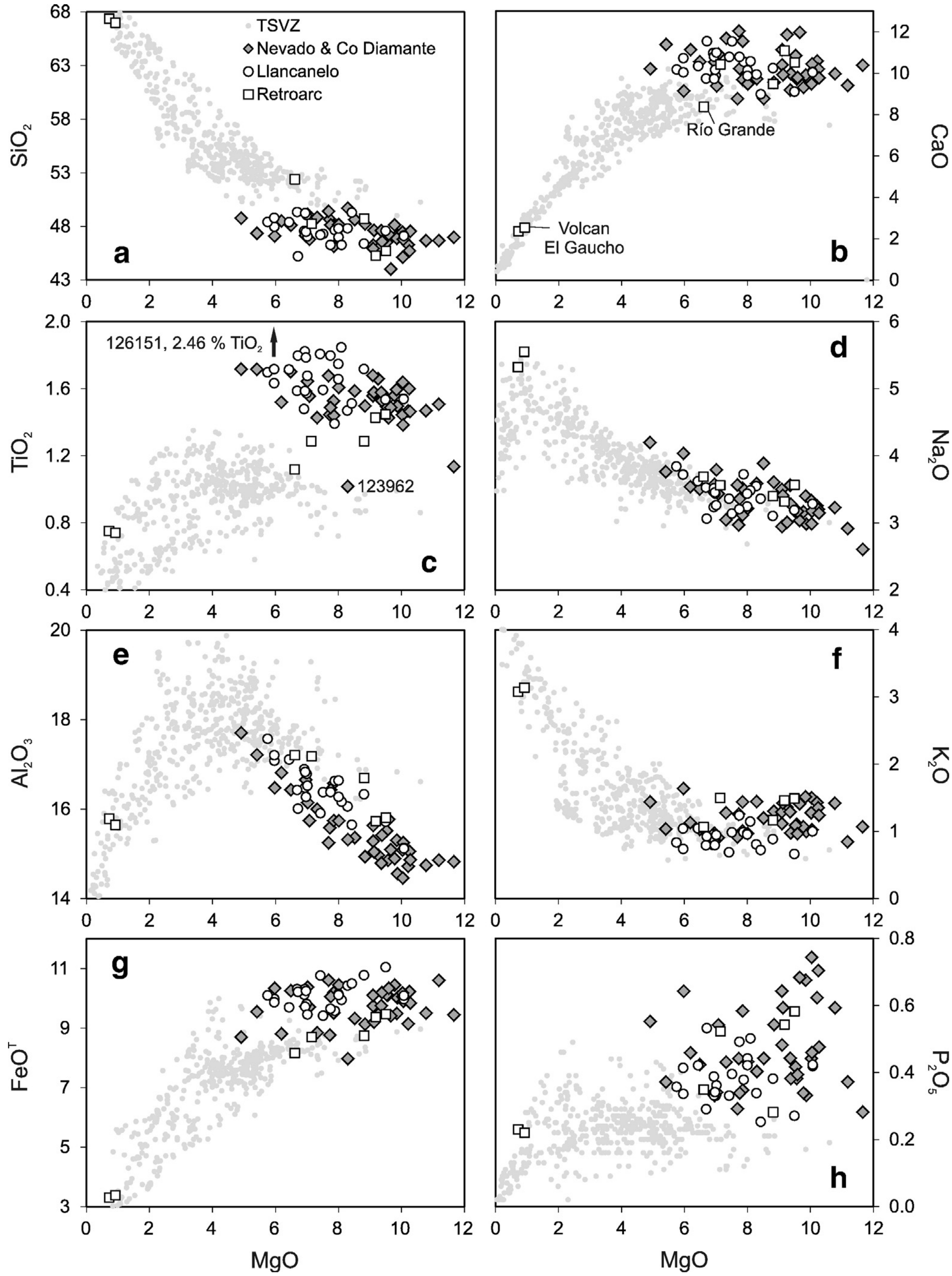

Fig. 3. a–h: MgO vs. SiO_2, CaO, TiO_2, Na_2O, Al_2O_3, K_2O, FeO^T and P_2O_5 for the northern Payenia and Andes retroarc samples. Data from Andes TSVZ have the same references as in Fig. 2. FeO^T is all iron calculated as FeO. Major elements have been recalculated on a volatile free basis.

sample 126174 from the Río Colorado volcanic field has a trace element pattern similar to the Nevado basalts with negative Nb–Ta anomaly and positive Pb-anomaly.

6.3. Sr and Nd isotopes

The Sr and Nd-isotopic ratios of the Nevado basalts (Fig. 9) largely fall within the range of the TSVZ rocks and form a negatively correlated trend similar to the TSVZ data. The Payún Matrú basalts similarly form a negatively correlated trend which apparently cross-cuts the Nevado trend and this was explained as due to crustal contamination by Pasquarè et al. (2008). The samples from the Payún Matrú, Río Colorado and Auca Mahuida region (Kay, 2001; Kay et al., 2004) range down to lower $^{87}Sr/^{86}Sr$ at a given $^{143}Nd/^{144}Nd$ than the Nevado basalts.

7. Discussion

7.1. Fractional crystallisation of the Payún Matrú basalts

Although hybrid magmas produced by magma mixing between primitive and evolved compositions are found in the early products of the Payún Matrú complex (Hernando et al., 2012) the intermediate basaltic compositions of many Payún Matrú lavas cannot be explained by mixing between the most primitive erupted basaltic magmas and a trachytic magma because they do not plot on straight mixing lines

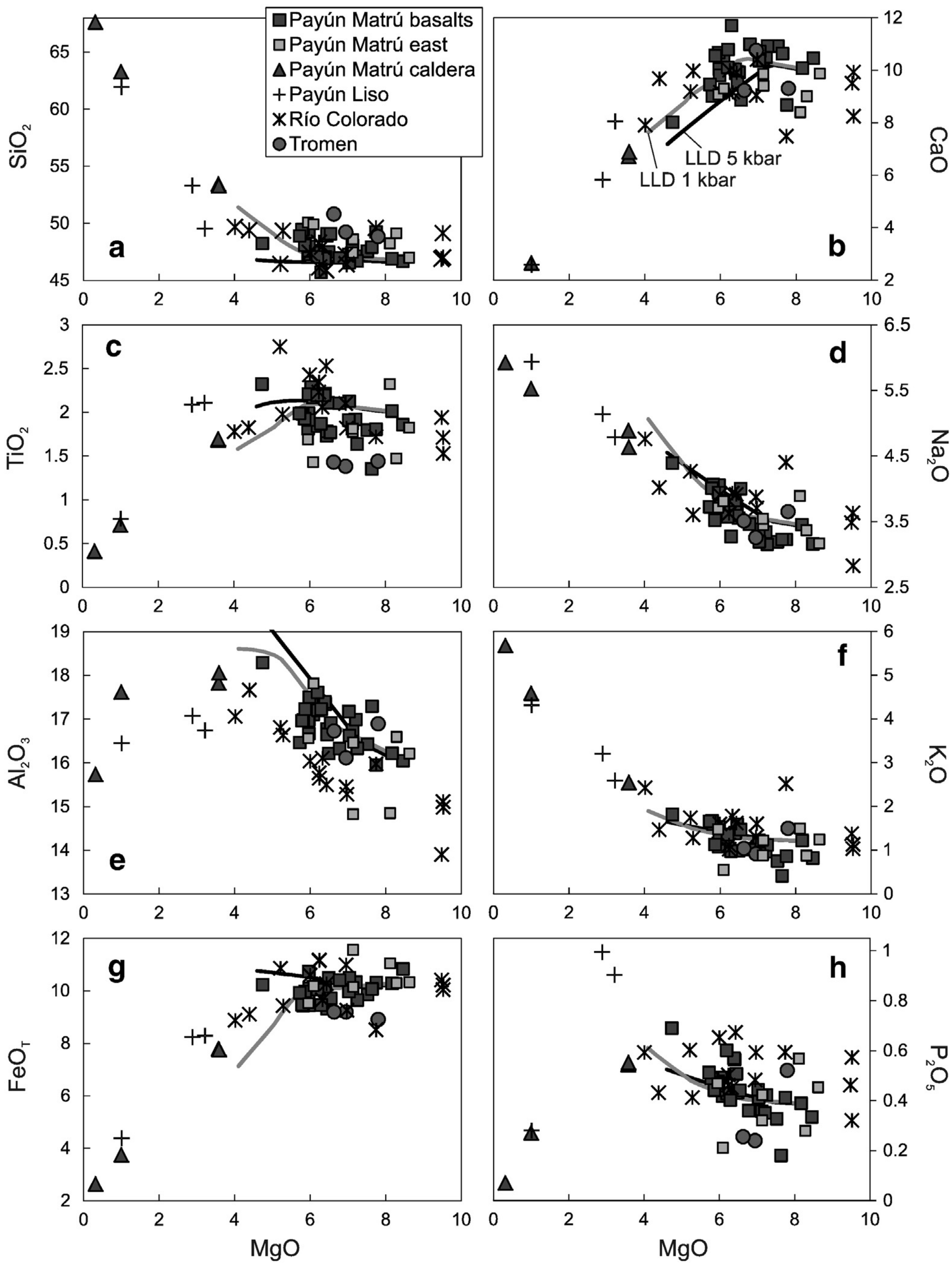

Fig. 4. a–h: MgO vs. SiO_2, CaO, TiO_2, Na_2O, Al_2O_3, K_2O, FeO_T and P_2O_5 for the southern Payenia samples. The older samples erupted from the eastern part of the Carbonilla fracture, called Payún Matrú east, have been plotted separately. The 5 kbar (black) and 1 kbar (grey) lines are the modelled liquid lines of descent for fractional crystallisation at 5 and 1 kbar respectively of sample 123936, modelled with MELTS software (see text for discussion and references). The Río Colorado sample 126175 with 13.1 wt.% MgO is outside the shown MgO range.

between the two end-members in Figs. 4 and 6a. Instead, the magmatic trends may have been formed by fractional crystallisation. Two liquid lines of descent reproducing the trends of the basaltic magmas have been modelled in MELTS (Ghiorso and Sack, 1995; Asimow and Ghiorso, 1998; Smith and Asimow, 2005) using sample 123936 with Mg# = 64, 113 ppm Ni and 234 ppm Cr as a model parental magma composition (Figs. 4 and 6). This sample plots at the high Mg#/MgO ends of the trends formed by the Payún Matrú basalts which may have been derived from magmas similar to this. Since the composition of sample 123936 is not in equilibrium with mantle olivine, the primary magmas must have fractionated olivine at an earlier stage, possibly at lower crustal levels, before ascent and eruption or further fractionation. The first model is at 5 kbar with 1.5% H_2O and fO_2 set to +1 FMQ. This is to investigate the possibility of fractionation at mid-crustal levels which was indicated by clinopyroxene thermobarometry on Pampas Negras lavas (Lauritsen, 2010). In this model, olivine crystallises and after 2% fractionation, clinopyroxene and spinel join the assemblage in the relative proportions ol:cpx:sp = 3.5:95:1.5. In this model, the fractionation from ~6 wt.% MgO to the evolved Payún Matrú magmas would have happened at lower pressure in order to have plagioclase in the crystallising assemblage.

The second model at 1 kbar with 1% H_2O and fO_2 set to +1 FMQ explores the possibility that all fractionation in the observed MgO-range took place at shallow levels. The increase in Al_2O_3 and Sr with decreasing Mg# and MgO among the Payún Matrú basalts (Figs. 4e and 6a) precludes plagioclase as a fractionating phase at

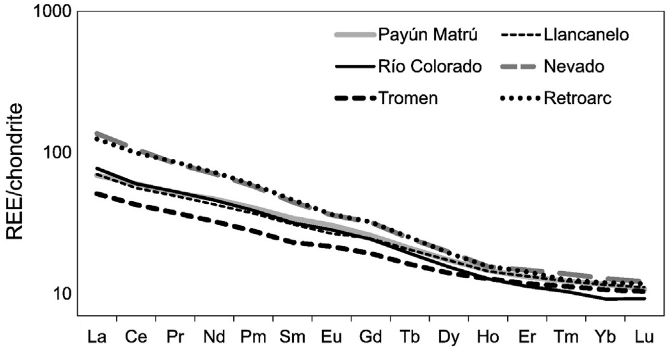

Fig. 5. REE patterns of representative primitive basalts from the main sample groups normalised to CI chondrite (McDonough and Sun, 1995).

this stage. In this model, olivine crystallises first followed by 5% spinel + 95% olivine after ~2% fractionation. At 6.5 wt.% MgO, clinopyroxene starts crystallising along with spinel and olivine in the respective proportions 94:2:4. Only at 5.2 wt.% MgO, does plagioclase join the fractionating assemblage. The large, partly resorbed plagioclases commonly found in the Los Volcanes and Pampas Negras basalts (see Section 4) are therefore probably xenocrysts which could be derived from older crystal cumulates. However, assimilation of plagioclase xenocrysts cannot be responsible for the general major and trace element trends formed by the Payún Matrú basalts but may have caused some of the scatter around these trends. The second

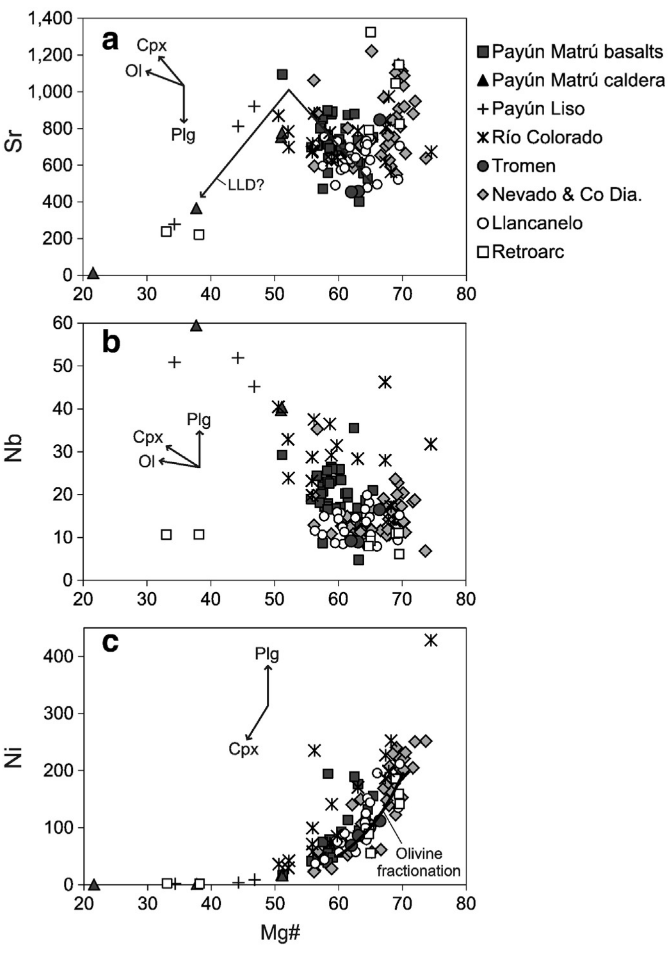

Fig. 6. a) Sr vs. Mg#, b) Nb vs. Mg#, and c) Ni vs. Mg#. The arrows show the effect of fractionation of olivine (ol), clinopyroxene (cpx) and plagioclase (plg). In a) a possible liquid line of descend (LLD) for the Payún Matrú rocks is outlined. The Payún Matrú basalts include the Payún Matrú east basalts.

model more accurately accounts for the trends of the Payún Matrú basalts but fractionation may well have happened at multiple levels in the crust. Furthermore, the considerable scatter around the overall trends in some elements, i.e. CaO and TiO_2, suggests a significant variation in the primitive magma compositions as is also reflected in the trace element ratios (Fig. 8). This is primarily related to a difference between the mainly older Payún Matrú east flows and the younger lavas from Los Volcanes and Pampas Negras. However, the magmas apparently followed very similar fractionation paths.

7.2. Lower crustal contamination of Payenia rocks

A common feature of samples from both the Northern Segment, Nevado, Llancanelo, Payún Matrú and Río Colorado volcanic fields are trends towards high Ba/Th, Nb/U and Eu/Eu* ($Eu/Eu^* = Eu_N / \sqrt{(Sm_N \cdot Gd_N)}$), intermediate Ba/Nb and Ce/Pb, and low U/Pb, Cs/Rb and Th/La (Figs. 8 and 10). Such trace element characteristics are distinctly different from the SVZ arc rocks and felsic upper continental crust (UCC, Rudnick and Gao, 2003) which both typically have low Nb/U and Ce/Pb, negative Eu-anomalies, high Th/La and Cs/Rb and high contents of Pb. Instead, they are characteristic for feldspar-bearing depleted lower crust (LCC, Rudnick and Gao, 2003) and we therefore consider it likely that these samples have been affected by lower crustal contamination. Among the samples from the Payún Matrú volcanic field it is mainly the Payún Matrú east lavas (included in the Payún Matrú group in Fig. 8) and the sample 126239 from Cara Cura that appear to have assimilated lower crust (Fig. 8). The feldspar imprint on the trace element patterns of these samples, i.e. positive Ba, K, Sr and Eu anomalies, speaks against an origin in the lithospheric mantle for the contaminating melts because feldspar is not stable here. The Ce/Pb ratios indicated for the contaminants by the high Ba/Th samples in Fig. 8b (>13) is higher than the LCC average (5) of Rudnick and Gao (2003) which may suggest a lower content of Pb in the local lower crust as is also indicated for the high Ba/Th end-member of the trend in Fig. 10a.

The increasing Ba/Th indicating increasing degrees of lower crustal contamination is accompanied by a decrease in the content of all incompatible elements (Fig. 10) including Ba and Sr as well as La/Sm and La/Yb, whereas Lu/Hf increases. Therefore the contaminating rocks or melts must have been highly depleted and have had considerably lower contents of incompatible elements than the mantle melts which argues against silicic small degree partial melts of lower crust. The decreasing trace element contents and La/Sm and increasing Ba/Th are in turn correlated with decreasing $^{143}Nd/^{144}Nd$ and increasing $^{87}Sr/^{86}Sr$ in the Nevado basalts (Fig. 11c, d and f). The plots in Fig. 11 focus on the Nevado basalts because the majority of the Nevado samples display a regular variation towards a composition similar to the LCC. The positive Eu/Eu* indicated for the lower crustal contaminant of the Nevado basalts at low Mg# and Th concentrations (Fig. 11h) requires that plagioclase was completely melted out of the source because residual plagioclase would cause the contaminating melts to have negative Eu-anomalies and lower Ba/Th due to the high $D_{Ba/Th}$ in plagioclase. So either the plagioclase content of the lower crust was low or the degree of melting of this crust was high which could also be attained by bulk assimilation.

The variations in trace element ratios indicative of lower crustal contamination, e.g. Ba/Th, La/Yb and Eu/Eu*, and the contents of incompatible trace elements in the Nevado group are correlated with variations in the major element contents. For example, there is a positive correlation between Mg# and Th and La/Yb (Fig. 11a and b) and a negative correlation between Mg# and Eu/Eu* (Fig. 11h), except for some of the samples containing clinopyroxene and/or plagioclase in addition to olivine phenocrysts (marked with black dots). Some of these samples may be somewhat evolved by fractional crystallisation but most of them plot along with the samples that only contain olivine phenocrysts. The Nevado basalts therefore form trends highly

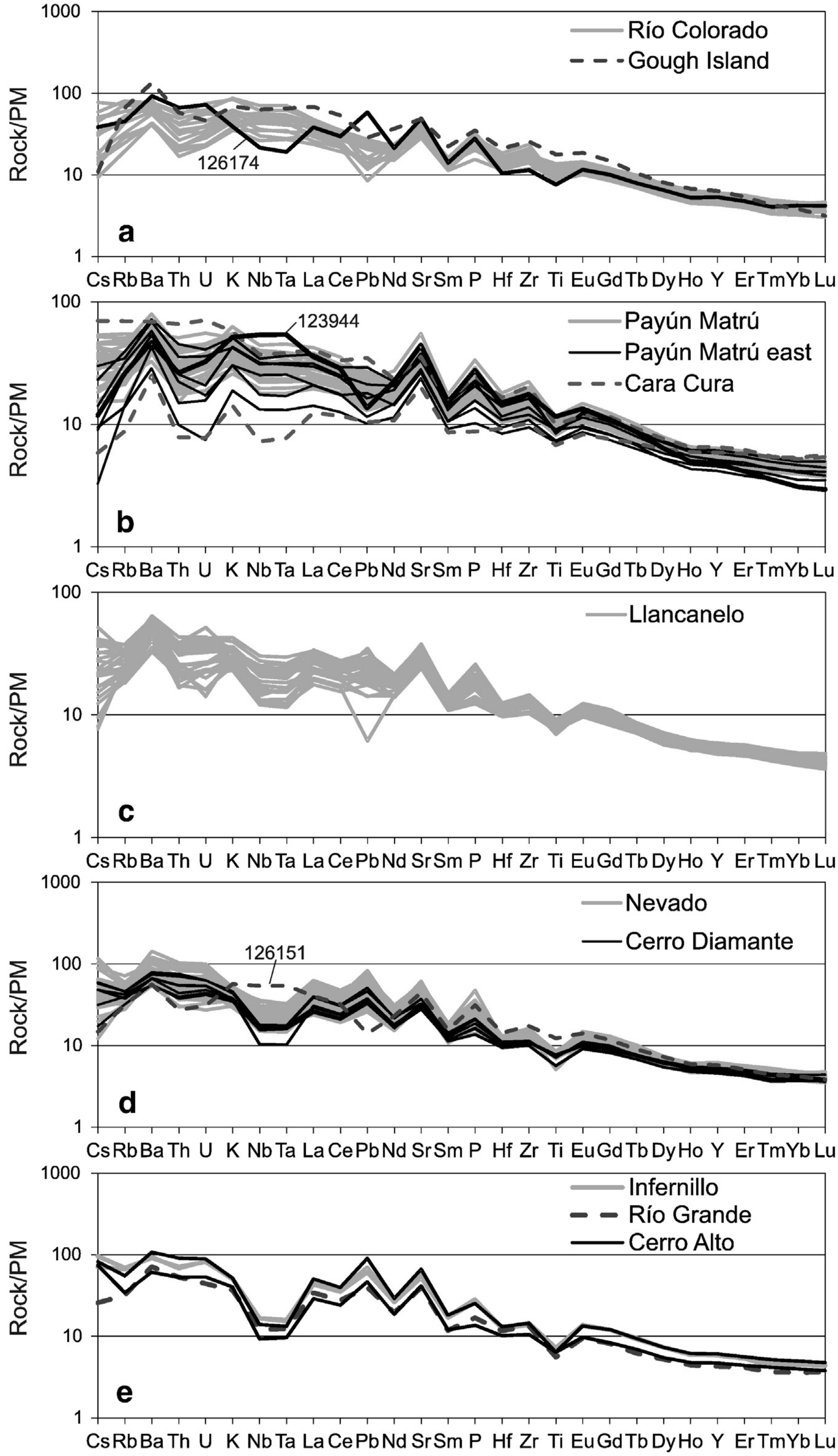

Fig. 7. Spider diagrams of basaltic samples from the five subgroups: a) Río Colorado. Sample 126174 is highlighted because it differs from the rest and is similar to the Nevado basalts. b) Payún Matrú volcanic complex and Cara Cura. Sample 123944 from Payún Matrú east is highlighted because it differs from the rest and is similar to the Río Colorado basalts. c) Llancanelo. d) Nevado and Cerro Diamante. Sample 126151 is highlighted because it differs from the rest and is similar to the Río Colorado basalts. e) Andes retroarc. The Gough Island sample in panel a is from Willbold and Stracke (2006). Samples in panel e are normalised to primitive mantle values from McDonough and Sun (1995)

oblique to what is expected from fractional crystallisation of olivine (and clinopyroxene and plagioclase). This suggests that the trends are two component mixing lines between the primitive mantle melts and the lower crustal contaminant. Considering the large effect 10% olivine fractionation has on the Mg#, the relatively well constrained mixing trends in Fig. 11a, b and h indicates very small amounts of fractionation for most Nevado samples. The contaminating melts must have had lower Mg# than the mantle melts but the steep trends in Fig. 11a and b indicate that they did not have much lower Mg# than the shown mafic lower crustal xenoliths from the

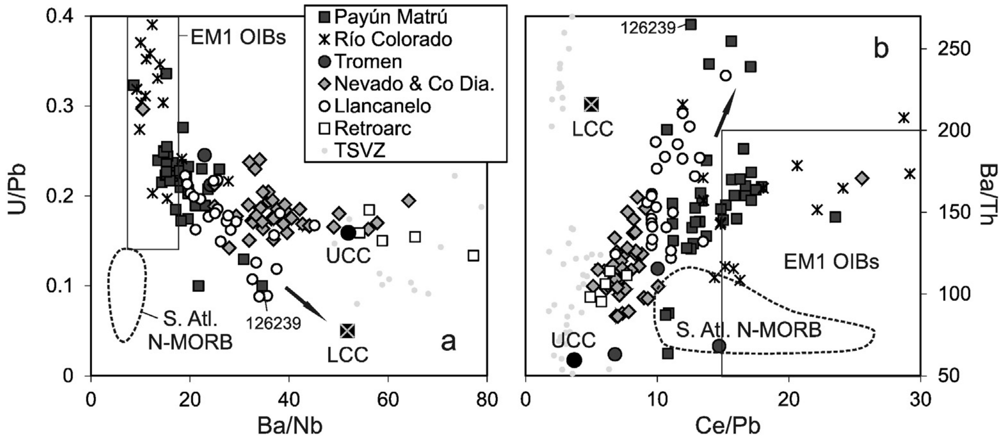

Fig. 8. a) U/Pb vs. Ba/Nb and b) Ba/Th vs. Ce/Pb for the basaltic Payenia samples. The Payún Matrú group includes the Payún Matrú east basalts. UCC and LCC are the upper and lower continental crust averages respectively (Rudnick and Gao, 2003). The arrows outline the trends towards a high Ba/Th–low U/Pb component which may have been caused by lower crustal contamination. Data from Andes SVZ have the same references as in Fig. 2. The squares show the range of trace element ratio values found in EM1 OIBs according to Willbold and Stracke (2006). The MORB field is based on south Atlantic N-MORB data ($(La/Sm)_N < 1$) from Humphris et al. (1985), Hanan et al. (1986), Fontignie and Schilling (1996), Douglass et al. (1999), le Roux (2000), Le Roux et al. (2001, 2002) and Agranier et al. (2005)

northern Cuyania terrane (Kay et al., 1996) which also forms the basement of the San Rafael block where the Nevado volcanic field is situated (see map in Ramos, 2004). Therefore the contaminating crust must have been mafic in order to generate basaltic melts.

In Fig. 11d and e, a mixing model for the Nevado basalts is shown as an attempt to estimate the amount of lower crustal assimilation necessary to explain the geochemical variation in these samples. The mixing lines are made between the possibly uncontaminated Nevado sample 123940 and a constructed lower crustal component (see details in Fig. 11 caption). The model suggests incorporation of up to ~70% bulk LCC in the magmas which is an extremely high percentage. Since the uncontaminated primitive mantle melts probably had varying contents of incompatible trace elements due to variations in degree of mantle melting and source enrichment, as is indicated in Fig. 10 and in the large range of Th contents at high Mg# in Fig. 11a, the modelled amount of assimilated crust will vary depending on which sample is used as the primitive melt. Also the composition of the actual assimilating melt is unknown but using isotope and trace element values similar to real lower crustal rocks, the modelled percentages will in all cases be very high (~60–70%). The amount of lower crustal assimilation in the high Ba/Th rocks from the other volcanic fields in Payenia is harder to define, but judging from the large variations in trace element ratios (Figs. 8 and 10), the amount may in some cases be similarly high here.

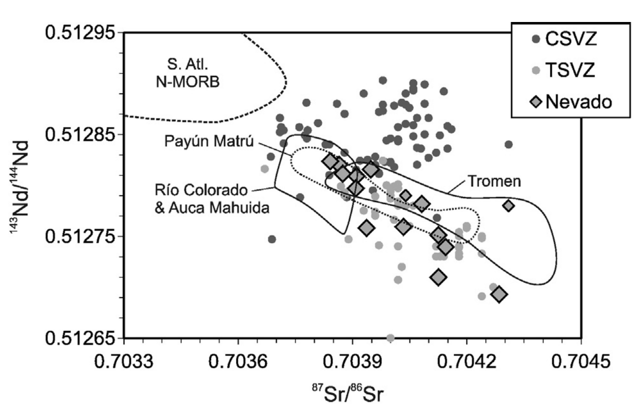

Fig. 9. $^{143}Nd/^{144}Nd$ vs. $^{87}Sr/^{86}Sr$ for twelve Nevado basalts. The small Nevado symbols are data from Stern et al. (1990) and Muñoz Bravo et al. (1989). Data references for southern Payenia rocks: Pasquarè et al. (2008), Españon (2010) (Payún Matrú), Kay (2001), Kay et al. (2004) (Río Colorado and Auca Mahuida) and Kay et al. (2006a) (Tromen). Data from Andes Central and Transitional Southern Volcanic Zone (CSVZ and TSVZ) are from http://georoc.mpch-mainz.gwdg.de and from Varekamp et al. (2006) and Holm et al. (in prep.)

For comparison with the mixing model, an AFC model has been shown in Fig. 11c and e with the same end-member compositions used as in the mixing model and with different rates of assimilation relative to fractionation (r). The only fractionating mineral is olivine in which the trace elements are highly incompatible. To obtain a decrease in the concentration of Th and La (and other highly incompatible elements) in the modelled melt compositions, requires r values > 1 and to model the trend of the Nevado basalts, r must be at least 3. However, the modelled melts have assimilated 300% crust when the Th concentrations reaches 2.5 ppm ($r = 3$, $F = 3$) so the AFC-model cannot provide a reasonable constraint on the amount of assimilated crust. Reiners et al. (1995) showed that very high r-values (>3) can be obtained in the earliest stages of fractionation when only olivine is on the liquidus or at temperatures above the liquidus because the change in magma composition caused by the assimilation supresses crystallisation at this stage (Bowen, 1922). In this way, large amounts of crust can be assimilated with very little crystallisation of olivine and this will result in large changes in trace element and isotopic composition with only minor changes in the major element contents. The amount of crust assimilated during this stage increases with increasing temperature of the crust and with increasing H_2O-content in the magma due to a depression of the plagioclase saturation temperature and expansion of the olivine stability field (Reiners et al., 1995). Since most of the Nevado basalts are highly primitive (high Mg#) and supposedly had high H_2O-contents, they might have assimilated hot lower crust by this type of process, possibly almost entirely above the olivine liquidus. This would explain why the majority of the Nevado samples fall on the positively correlated trends in plots of Mg# vs. incompatible trace elements (for example Figs. 6a and b and 11a and b) and not on trends expected from fractional crystallisation.

The variations seen in the Nevado basalts are very similar to what was described for the alkaline Pisgah volcano in California by Glazner et al. (1991). These authors found decreasing incompatible element contents with decreasing MgO and $^{143}Nd/^{144}Nd$ and increasing $^{87}Sr/^{86}Sr$ (Fig. 11) and this was ascribed to assimilation of significant amounts of high-degree partial melts of depleted mafic lower crust (gabbros or mafic granulites). During the short lifetimes of each volcano, the erupted magmas changed from nearly pure mantle melts to nearly pure remelted mafic crust and this was explained as due to differential tapping of a

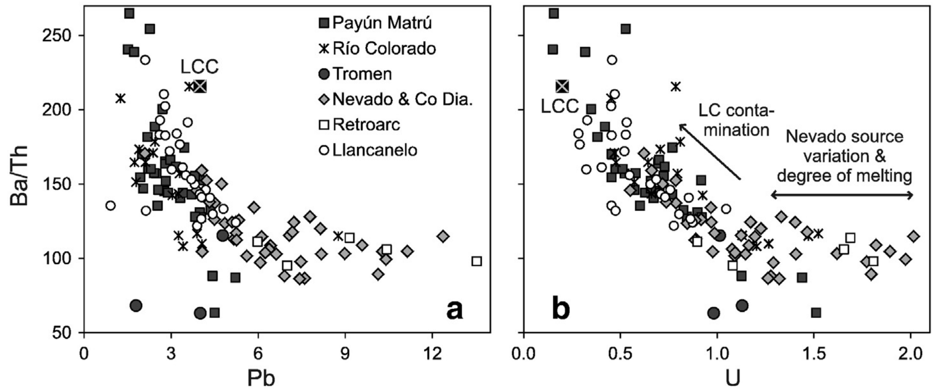

Fig. 10. a) Ba/Th vs. Pb and b) Ba/Th vs. U. Except for the Tromen volcanic field, all groups of basaltic Payenia samples form trends towards compositions similar to the global lower continental crust average (LCC, Rudnick and Gao, 2003) with very high Ba/Th and low contents of incompatible elements such as U and Pb. In comparison, the average upper continental crust has a Ba/Th of 59, 17 ppm Pb and 2.7 ppm U (Rudnick and Gao, 2003) and are outside the plots. The Nevado samples show a significant variation in trace element contents at relatively constant Ba/Th and this is can be related to varying source enrichment and degrees of melting. The Payún Matrú basalts include the Payún Matrú east basalts.

stratified magma chamber where only the uppermost part of the magma body contained large amounts of assimilated lower crust. The authors proposed that repeated injections of hot basaltic magmas were enough to create a zone of partially melted rock in the lowermost crust (a MASH-zone Hildreth and Moorbath, 1988) where the crust was melted to a high degree.

According to the gravity model of Tassara et al. (2006) the lithosphere in the Payenia region is thin, ~60–80 km, while the crust is relatively thick, 40–50 km (e.g. Gilbert et al., 2006; Tassara et al., 2006; Alvarado et al., 2007; Mazzarini et al., 2008). Thus the lithospheric mantle must be very thin and much thinner than expected from the Greenvillian age of the Cuyania terrane (Kay et al., 1996). The lithospheric mantle may have been thinned recently due to erosion by the asthenospheric corner flow which must have been shifted eastwards during the shallow subduction period in the Miocene–Pliocene period. This would have caused an increased conductive heating of the lower crust and facilitated its melting. However, too little time has elapsed for such heating from below to have had an effect on the geotherm in the middle and upper crust (Turcotte and Schubert, 2002). Furthermore, the lower crust may locally have been preheated by the intensive arc and back-arc volcanism that occurred in parts of the province during the late Miocene and Pliocene, in particular in the Sierra de Palauco and Payún Matrú regions in the central depression and in the Nevado volcanic field (e.g. Yrigoyen, 1993; Nullo et al., 2002; Litvak et al., 2008), for example by igneous underplating. Possibly the continuous injections of hot magmas into an already hot lower crust was sufficient to melt the crust in large parts of the province and the lavas indicating the very high degrees of contamination may only represent small portions of the magma batches as suggested by Glazner et al. (1991) for the Pisgah volcano in California.

Another possible explanation for the apparently large amount of lower crustal melt in some Payenia basalts could be that the assimilated component of lower crust was derived from the arc or fore-arc, either by delamination or subduction erosion. Subduction erosion has been shown to be an important process in the northern Southern Volcanic Zone (NSVZ) due to the strong compressional tectonics caused by the Pampean flat slab (Stern, 1991, 2011; Stern and Skewes, 1995; Kay et al., 2005; Stern et al., 2007, 2011). Likewise, the Miocene to Pleistocene shallow subduction zone in the Payenia region may have enhanced the subduction erosion and caused a source region contamination with lower crustal rocks beneath the province. It is very difficult to distinguish this type of mantle process from crustal contamination within the lithosphere, but mafic lower crustal rocks would be expected to be garnet-bearing at sub-lithospheric depths and thus result in a strong depletion in heavy REE in the magmas. High La/Yb (15–55) and low Yb contents in Miocene–Pliocene rocks from the NSVZ led Kay et al. (2005) to conclude that the magmas equilibrated with garnet-bearing crustal rocks either in the mantle or the deep crust. In comparison, the La/Yb of the Nevado basalts decreases to <9 in the most contaminated basalts (Fig. 11b) and shows no indication of equilibration with residual garnet. Furthermore, if the lower crust was recycled into the mantle and melted on top of the slab, the lower crustal signature would be expected to be accompanied by a contribution from slab and sediment fluids or melts but this is not the case. In particular the Río Colorado and Payún Matrú basalts do not appear to contain such components. It is also unlikely that source contamination by lower crustal material has happened on such a large scale as there is indication of lower crustal contamination in almost all volcanic fields in Payenia. Therefore the lower crustal contamination probably happened within the local crust.

7.3. Geographical variations in the volcanism and contributing source components

The Payún Matrú basalts are apparently derived from the same mantle source as the Río Colorado basalts because they have very similar trace element ratios and patterns and similar Sr–Nd-isotopes (Figs. 7, 8, 9 and 12). The La/Nb and Ba/Nb ratios of the Payún Matrú basalts were never as high as in the Nevado volcanic field to the east although the Payún Matrú volcano is positioned closer to the arc, and there is no indication of a decrease in these values with time. Therefore this volcanic system does not seem to have received a decreasing slab input during Pleistocene times like the Tromen volcano (Kay et al., 2006a) despite the fact that arc-like lavas were erupted during the same period just north of Los Volcanes in the Río Grande region (here part of the retroarc group) (Fig. 1). In contrast to the Payún Matrú east basalts, the Los Volcanes and Pampas Negras basalts (LV and PN on Fig. 1) (except for the older sample 126255 with very high Ba/Th) (all part of the Payún Matrú group) do not trend towards the lower crustal compositions. In trace element space, these samples generally form trends from the Río Colorado samples towards compositions similar to the arc rocks or upper crustal compositions for example by increasing La/Nb, Ba/Nb, Th/Nb and Th/La and decreasing U/Pb, Ce/Pb and Nb/U (Fig. 8). This could be caused by small amounts of enrichment with slab fluids, either by direct fluid addition to their source mantle or through melting of metasomatised lithospheric mantle, or it could be caused by assimilation of more felsic continental crust. These two processes are hard to separate but if the trends have been caused by upper crustal contamination, the amount of assimilated rock must be very small, as was

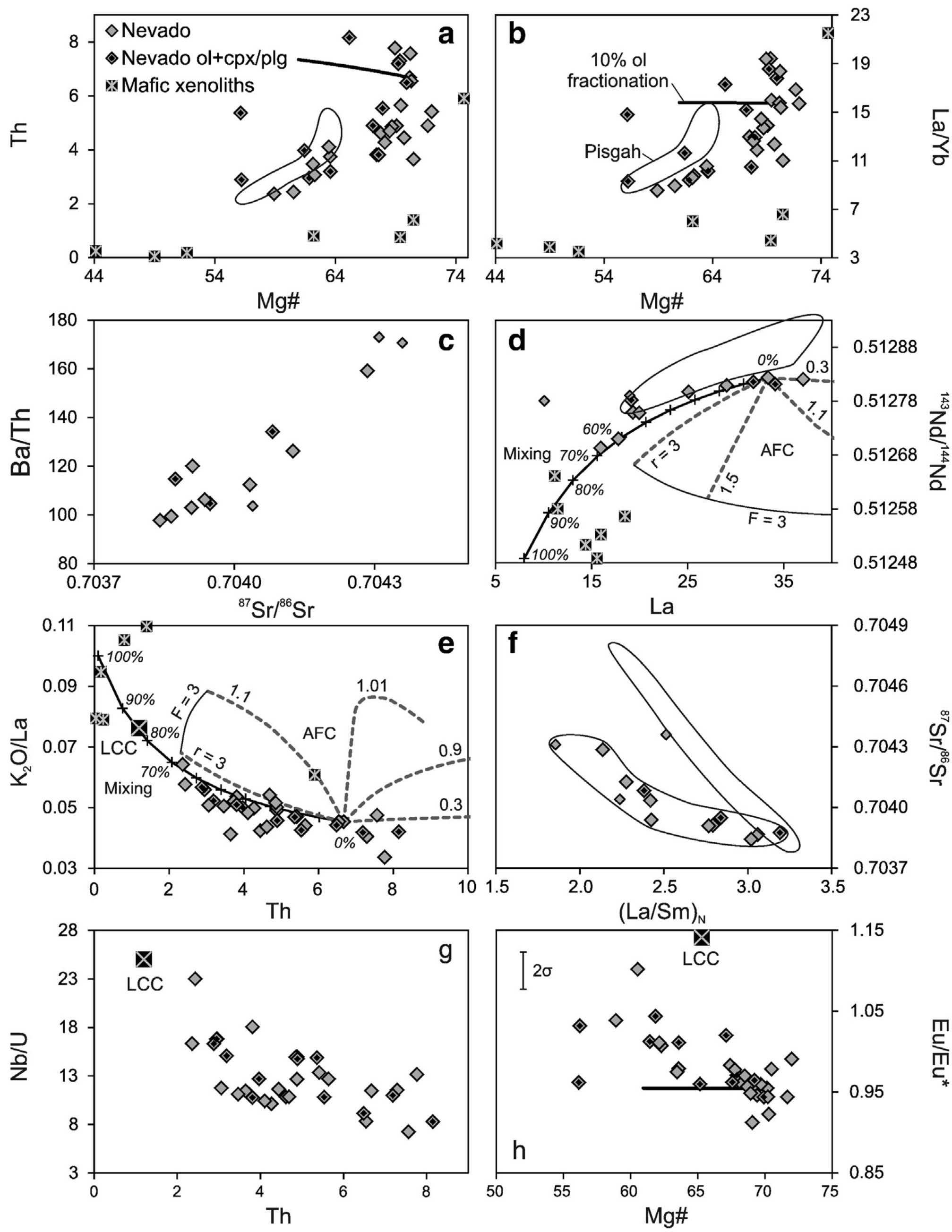

Fig. 11. Modelling of lower crustal contamination of the Nevado basalts. a) Th vs. Mg#, b) La/Yb vs. Mg#, c) Ba/Th vs. $^{87}Sr/^{86}Sr$, d) $^{143}Nd/^{144}Nd$ vs. La, e) K_2O/La vs. Th, f) $^{87}Sr/^{86}Sr$ vs. $(La/Sm)_N$ (normalised to chondrite values from McDonough and Sun (1995)), g) Nb/U vs. Th and h) Eu/Eu* vs. Mg#. The Nevado samples containing clinopyroxene (cpx) and/or plagioclase (plg) in addition to olivine phenocrysts are marked with black dots. Only six of these contain plagioclase phenocryst (0.5–6% of total rock). The black lines in a), b) and c) show the effect of 10% olivine fractionation. The mafic xenoliths are lower crustal basement xenoliths from the northern Cuyania terrane (Kay et al., 1996). The small Nevado symbols in d) and f) are data from Stern et al. (1990) and Muñoz Bravo et al. (1989). The fields outlined in black in a), b), d) and f) show data from the Pisgah volcano in California (Glazner et al., 1991) which have also been ascribed to lower crustal contamination. Data from Kay et al. (1996) and Glazner et al. (1991) do not include Nb and Gd. The 2σ bar in h) shows the standard deviation on the measured Eu/Eu* for the DISKO-1 standard (2σ = 4.6 relative %) (Electronic Appendix B). Standard deviations for the BHVO-2 and BCR-2 measurements are lower (2σ = 4 and 2.8 relative % respectively). The mixing models (black lines with crosses) shown in d) and e) are calculated using the Nevado sample 123940 with La = 33.4 ppm, Nd = 33.6 ppm, Th = 6.7 ppm, K_2O = 1.51 wt.% and $^{143}Nd/^{144}Nd$ = 0.512824 and a constructed lower crustal end-member with La = 8 ppm, Nd = 11 ppm (both adopted from the global lower crustal average of Rudnick and Gao, 2003), Th = 0.1 ppm, K_2O = 0.8 wt.% and $^{143}Nd/^{144}Nd$ = 0.512488. Percentages state the amount of lower crust in the mixture. The grey dashed lines in d) and e) are AFC models with the same end-member compositions as in the mixing model and with varying r values (rate of assimilation relative to rate of fractionation). For high r values, the AFC curves approach the mixing curves but it requires unrealistically high degrees of fractionation and assimilation (F = 3) to reach the most contaminated Nevado samples. The only fractionating mineral is olivine with partition coefficients from Kennedy et al. (1993) (La = 0.00028, Nd = 0.0002, Th = 0.00021) and Philpotts and Schnetzler (1970) (K_2O = 0.0056).

also concluded from the variation of the $^{87}Sr/^{86}Sr$ ratios in the Payún Matrú rocks (Hernando et al., 2012) (Fig. 9).

The Río Colorado mantle source is apparently an asthenospheric mantle component but with a trace element composition noticeably different from normal MORB asthenosphere. The higher Ba/Nb (~10) and Sr/Nd (~25–32) of this source compared to N-MORB cannot have been caused by addition of slab components, because the Río Colorado lavas have higher U/Pb (0.2–0.4) (Fig. 8) and lower La/Nb than

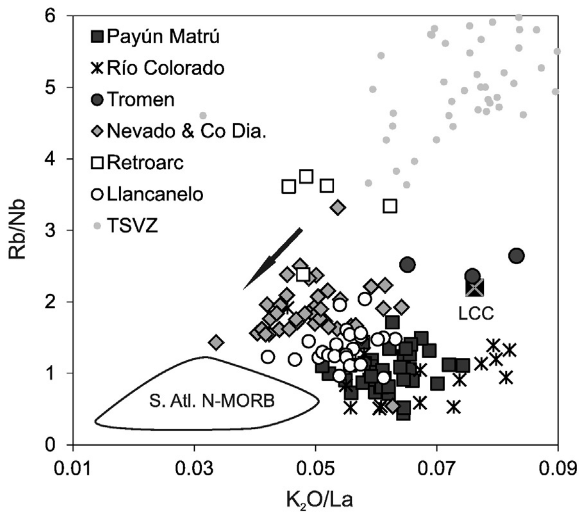

Fig. 12. K_2O/La vs. Rb/Nb. The arrow emphasises the trend of the Nevado, Cerro Diamante, retroarc and TSVZ rocks towards low, MORB-like K_2O/La and Rb/Nb. The southern Payenia basalts have higher K_2O/La and lower Rb/Nb than the northern Payenia basalts. References for Andes TSVZ and South Atlantic N-MORB are the same as in Figs. 2 and 7. The Payún Matrú basalts include the Payún Matrú east basalts. LCC is the lower continental crust average from Rudnick and Gao (2003).

N-MORB and as low Th/Nb as depleted Pacific MORB (e.g. Bach et al., 1996), contrary to what is expected by addition of aqueous fluids or melts from subducted material. Moreover, the negative Pb anomalies in primitive mantle normalised trace element patterns and high Ce/Pb ratios of the Río Colorado basalts (Fig. 8), preclude any significant influence from subduction components or crustal contaminants. Instead, the Río Colorado lavas have trace element patterns similar to EM-1 OIBs (Zindler and Hart, 1986) such as Gough Island. Therefore the Río Colorado basalts are intraplate basalts unrelated to the subduction zone as also noted by Kay et al. (2006a) and the volcanism in the Río Colorado and Payún Matrú volcanic fields must have been instigated by other processes than slab fluid generated melting which dominates the Nevado and Northern Segment basalts. The Río Colorado mantle source may be related to the plume-like structure centred beneath Payún Matrú which was imaged in an E–W electrical conductivity profile across the Payún Matrú volcanic field (Burd et al., 2008) but it is still unclear what the nature and cause of this structure is. The southern Payenia basalts reflect the same mantle source composition since the late Pliocene, as evidenced by e.g. low La/Ta and Ba/Ta in Auca Mahuida and late Pliocene to Pleistocene Chachahuén basalts (Kay, 2001; Kay et al., 2004, 2006a) and samples from the cones and flows surrounding the Chachahuén complex (Bertotto et al., 2009, and this study). This indicates that the shallowly subducting slab retreated from the southern Payenia province already in the Pliocene (Kay et al., 2006a; Gudnason et al., 2012). The basalts from the Tromen volcanic field closer to the arc-front are an exception to this picture because the Tromen rocks in general apparently received an input from the subducting slab (Kay et al., 2006a). This input has decreased from the Pliocene to Recent times supporting the suggestion of a retreating slab (Kay et al., 2006a).

The late Pliocene and Pleistocene Nevado basalts and the upper Pleistocene Cerro Diamante basalts are transitional basalts in the sense of Stern et al. (1990) with compositions in between those of intraplate and arc lavas. The Ba/Ta (440–1156) and La/Ta (22–52) ratios are in the same range as the late Miocene high-K Chachahuén basalts (Kay et al., 2006b), suggesting a similar degree of slab component enrichment. The calc-alkaline Miocene Chachahuén volcanic rocks were interpreted to have formed ~180 km above the shallowly subducting slab due to the break-down of phlogopite in the descending slab (Kay et al., 2006b). The slab may have been at a similar depth below the San Rafael Block during the formation of the Nevado volcanic rocks in the lower Pleistocene as they are also high-K rocks, and the young geochemically similar Cerro Diamante volcano in the Northern Segment is presently ~180–190 km above the subducted Nazca plate (Cahill and Isacks, 1992). Therefore the Nevado, Cerro Diamante and Miocene Chachahuén basalts may have formed around the same height above the slab by similar melting processes. The northern Payenia volcanism can thus be regarded as backarc volcanism caused by the release of fluids or melts from a slab more shallow than the present day slab which is currently at a depth of ~250 km below the Cerro Nevado volcano. The age progression of the slab-fluid induced volcanism from the southern Nevado in the late Pliocene to the northern Nevado in middle Pleistocene times and further to the Northern Segment in the late Pleistocene is presumably linked to the progressive downwarping of the subducting slab from south to north and northwest (Folguera et al., 2009; Gudnason et al., 2012) so that the slab retreated in a direction oblique to the trench but far from perpendicular. Thus, the northern Payenia volcanism marks the end of the period of shallow subduction and the final roll back of the slab.

The nature of the asthenospheric mantle source for the northern Payenia basalts is not easily revealed due to the overprinting by the slab flux. However, these magmas cannot have been derived from the same mantle source as the southern Payenia basalts because they have lower K_2O/La than both the primitive arc rocks with $MgO > 5$ wt.% and the Río Colorado basalts (Fig. 12). Addition of aqueous fluids or melts from the subducting slab would be expected to increase the K_2O/La of mantle melts because K_2O is more fluid mobile than La, so the northern Payenia basalts should have had higher K_2O/La than the Río Colorado lavas if they were derived from the same asthenospheric mantle source as these. In Fig. 12 they extend the trend of the TSVZ samples towards the South Atlantic N-MORB data (samples with $(La/Sm)_N < 1$), and therefore they may have had a mantle source similar to the source of these N-MORB lavas but distinct from the source of the southern Payenia basalts. The existence of two distinct mantle sources is also indicated by the different isotopic compositions of the basalts since the least contaminated southern Payenia basalts have less radiogenic Pb and Sr than the northern Payenia basalts but similar Nd-isotopic compositions (Fig. 9) (Muñoz Bravo et al., 1989; Stern et al., 1990; Kay, 2001; Pasquarè et al., 2008; Hernando et al., 2012; N. Søager, unpublished data). However, the Nevado sample 126151 with a composition identical to the Río Colorado lavas, shows that this plume type mantle was occasionally present in this area as well. The Tromen samples plot between the Río Colorado and SVZ arc rocks and could, according to this plot, be derived from the Río Colorado source. The deviation from the main trend towards higher K_2O/La at constant Rb/Nb formed by some Nevado and Cerro Diamante samples is most likely caused by the lower crustal contamination and not because of mixing with the Río Colorado source, because these samples are the most contaminated (Fig. 11e). The Llancanelo rocks form a transitional group in Fig. 12 and in most other plots and the lavas have less slab-imprint than the Nevado basalts. Rather, they appear to contain inputs from all components in the system: the Río Colorado and MORB mantle sources, small amounts of slab fluids and abundant lower crustal contamination. The Llancanelo area therefore marks the transition between the shallow subduction related volcanism sourced by a normal MORB mantle in the northern Payenia province and the OIB-type intraplate volcanism prevailing in the southern part.

The Payenia volcanism thus seems to be related to the upwelling of enriched OIB-type mantle alongside normal MORB-type mantle after a period of shallow subduction. However, it is yet to be resolved what exactly the relationship between the subduction zone, the variation of the slab dip and the mantle upwelling in the Payenia province is and whether there is an additional driving mechanism for the mantle upwelling.

7.4. REE modelling of melting conditions

In Fig. 13, a model of the REE variations during mantle melting is used to estimate the depths and degrees of melting (F) of the basaltic samples from the dataset. The model is based on aggregated, incremental, non-modal batch melting of peridotite (Shaw, 1970) with a primitive mantle composition (McDonough and Sun, 1995), assuming that the melting happened as anhydrous decompression melting of an upwelling mantle. The porosity was defined as 0.3% and the garnet content of the source at high pressures was set to 10%. Melting modes and mantle source composition is based on McKenzie and O'Nions (1995). Mantle modes and partition coefficients are given in Electronic Appendix C. The mantle potential temperature (T_P) is given by the experimentally determined solidus pressures of peridotite based on the method of McKenzie and Bickle (1988). We emphasise that we cannot account for all complications in a simple model but the model gives a tool for a quantitative comparison of the samples. The model shows the initial melting pressures, P_i (black lines), which are the mantle solidus pressures, and the final melting pressures, P_f (green lines), where melting stops. To avoid the most crustally contaminated samples, only Nevado and Cerro Diamante samples with Ba/Th < 125 and Llancanelo, Payún Matrú and Río Colorado samples with Ba/Th < 180 have been plotted in Fig. 13.

If the model mantle source is further enriched, for example by addition of upper continental crust to the primitive mantle composition, the grid will mainly move towards higher $(La/Sm)_N$ and the modelled solidus pressures and degrees of melting will increase. But addition of as much as 10% continental crust will only increase the $(Tb/Yb)_N$ of the spinel-only curve ~0.1, so source enrichment cannot explain the high $(Tb/Yb)_N$ of the Payenia basalts. Instead, they must have been formed in the presence of garnet. The position of the samples in between the spinel-only and garnet-only curves suggests that the magmas were formed at the transition between spinel and garnet stability. The very low degrees of melting indicated for the Nevado, Cerro Diamante and retroarc samples, could suggest that they need a mantle source that is more enriched than the used primitive mantle. This could be due to enrichment by the slab flux. Still, the high $(La/Sm)_N$ ratios and low Zr/Nb (down to 6.3) and generally high content of incompatible elements (including Nb up to 23.6 ppm) of these samples, suggests relatively low degrees of melting, as also noted by Bermudez and Delpino (1989). This indicates that the asthenospheric mantle source was not hotter than average MORB mantle. The northern Payenia basalts have presumably been formed by flux fusion and as such, the model does not fully apply to these samples. Still, the $(Tb/Yb)_N$ of the magmas is controlled by the amount of garnet present during melting and the elevated $(Tb/Yb)_N$ ratios therefore require small amounts of garnet in the source.

The Río Colorado and Payún Matrú samples can presumably be modelled by anhydrous decompression melting. The Río Colorado samples plot at higher $(Tb/Yb)_N$ than the Payún Matrú and Llancanelo basalts. According to the model, the lower $(Tb/Yb)_N$ of the Payún Matrú and Llancanelo basalts relative to the Río Colorado and Nevado basalts may have been caused by a lower melt segregation pressure and hence a thinner lithosphere beneath the central depression in the western backarc than in the eastern part. This agrees with the model of Tassara et al. (2006) based on gravity data which suggested a lithospheric thickness of ~60–80 km for the Payenia area and a thinning of the lithosphere towards the west and south. The modelled final melting pressures for the Payenia basalts (2.7–2.83 GPa) are equivalent to a lithospheric thickness around 80–85 km which is close to the thickness estimated by Tassara et al. (2006).

The Río Colorado and Payún Matrú basalts indicate similar solidus pressures around 3 to 3.1 GPa corresponding to a T_P of ~1470–1480 °C in dry peridotite. This is considerably higher than average MORB mantle (1300–1400 °C, e.g. Herzberg et al. (2007)) and similar to what has been calculated for many mantle plumes (e.g. Herzberg and Asimov, 2008; Herzberg and Gazel, 2009). By decreasing the source enrichment in the model, the model grid will shift towards lower $(La/Sm)_N$ and the modelled solidus pressures and degrees of melting will decrease. However, it is not plausible that the Payún Matrú magmas were formed at much lower degrees of melting than the 2–5% indicated here. Therefore the modelled solidus pressures are rather considered minimum values. The high solidus pressures can also have been caused by a lower mantle solidus temperature due to enrichment of the source and/or to the presence of low solidus pyroxenitic lithologies in the mantle (e.g. Kogiso et al., 2004; Stracke and Bourdon, 2009). It is not at this stage clear what causes the high solidus pressures in the southern Payenia mantle but there must be a thermal or compositional mantle anomaly associated with this volcanism.

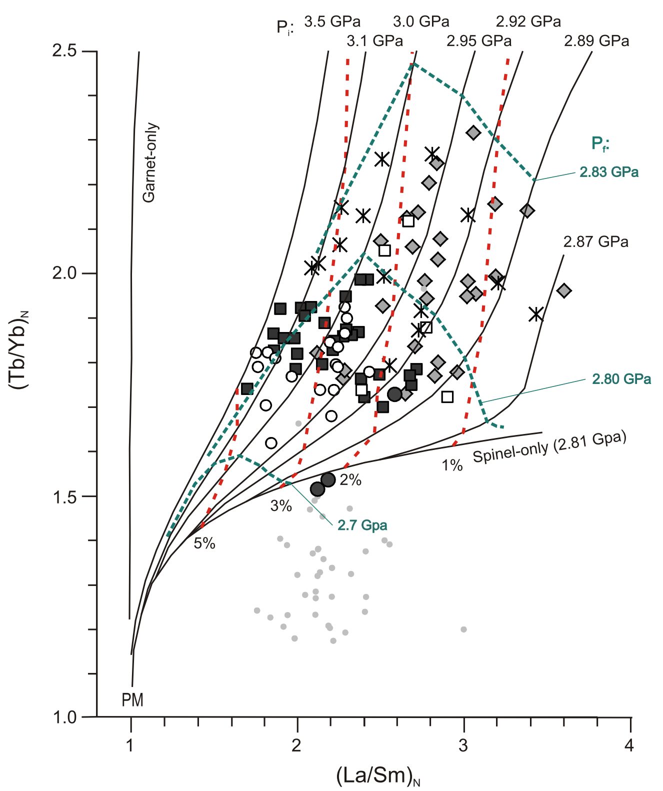

Fig. 13. $(La/Sm)_N$ vs. $(Tb/Yb)_N$ for the basaltic samples. Symbols and references as in Fig. 2 and 12. Only Nevado and Cerro Diamante samples with Ba/Th < 125 and Río Colorado, Payún Matrú and Llancanelo samples with Ba/Th < 180 have been plotted to avoid the lowest crustally contaminated samples. Black lines delineate melting paths from given solidus pressures indicated at the top of the figure as P_i, initial melting pressure. Green lines show depths of melting along the black curves indicating the final melting pressure, P_f, of the samples. Orange dashed lines mark the degree of melting, F. Details of the melting model are given in the text and in Electronic Appendix C. Only Andes samples with MgO > 5% are plotted. The Payún Matrú basalts include the Payún Matrú east basalts.
Chondrite normalisation values from McDonough and Sun (1995).

8. Conclusions

The southern Payenia basalts are alkaline intraplate basalts sourced by an EM-1 OIB-like mantle and, apart from the Tromen volcanic field samples, these basalts have had no or very little input from the subducting slab. This volcanism is associated with a thermal or compositional mantle anomaly which generates melts in a backarc environment. In contrast, the northern Payenia and retroarc lavas are ordinary backarc basalts formed by addition of fluids and melts from the subducting slab to a more MORB-like mantle source which was probably not hotter than average MORB mantle. This mantle may have been upwelling along with the southern intraplate mantle source during and after the retreat of the shallowly subducting slab. The shallowly subducting slab was probably at a depth of ~180–190 km beneath the Nevado volcanic field and Northern Segment at the time of magma formation in these volcanic fields and the Pleistocene shift in the San Rafael block volcanism from south to north and northwest marks the downwarping of the slab and the end of a shallow subduction regime. The Llancanelo lavas apparently formed at the transition between the southern Payenia intraplate volcanism and the northern Payenia backarc volcanism.

The REE melting model of the Payenia basalts shows that melting took place in the presence of small amounts of garnet and the modelled final melting pressures suggest a thinner lithosphere in the area of the central depression than in the eastern backarc beneath the Río Colorado and Nevado volcanic fields.

Trace element variations among the Payenia basalts suggest important melt contributions from lower crustal type rocks occasionally occurring in magmas from almost all parts of the province. The amount of contamination in the Nevado group lavas has been estimated to possibly up to 70% in the most extreme cases. The lower crustal contaminants must be depleted plagioclase-bearing mafic rocks.

Supplementary data to this article can be found online at http://dx.doi.org/10.1016/j.chemgeo.2013.04.007.

Acknowledgements

We thank the editor Laurie Reisberg and two anonymous reviewers for their comments to the manuscript which led to significant improvements. Jonas Gudnason, Mia Nielsen and Helene Heide Jørgensen are thanked for their assistance during field work, data analyses and thin section descriptions. We thank Jonas Gudnason and Charlotte Thorup Dyhr for making Ar/Ar ages of the samples and for many fruitful discussions. We would like to thank Jørgen Kystol, GEUS, for good collaboration and splendid analyses. Lars Nielsen is thanked for kindly discussing the geophysical aspects with us. We greatly acknowledge the support to PMH from the Danish Research Council for Nature and Universe grant 272-07-0514.

References

Agranier, A., Blichert-Toft, J., Graham, D.W., Debaille, V., Schiano, P., Albarede, F., 2005. The spectra of isotopic heterogeneities along the mid-Atlantic ridge. Earth and Planetary Science Letters 238, 96–109.

Alvarado, P., Beck, S., Zandt, G., 2007. Crustal structure of the South-Central Andes Cordillera and backarc region from regional waveform modelling. Geophysical Journal International 170 (2), 858–875.

Asimow, P.D., Ghiorso, M.S., 1998. Algorithmic modifications extending MELTS to calculate subsolidus phase relations. American Mineralogist 83 (9–10), 1127–1132.

Bach, W., Erzinger, J., Dosso, L., Bollinger, C., Bougault, H., Etoubleau, J., Sauerwein, J., 1996. Unusually large Nb–Ta depletions in north Chile Ridge basalts at 36°50′S to 38°56′S; major element, trace element and isotopic data. Earth and Planetary Science Letters 142, 223–240.

Bermudez, A., Delpino, D., 1989. La Provincia basáltica Andino-Cuyana (35°–37° L.S). Revista de la Asociación Geológica Argentina 44, 35–55.

Bermudez, A., Delpino, D., Frey, F., Saal, A., 1993. Los basaltos de retroarco extraandinos. In: Ramos, V.A. (Ed.), Geología y Recursos Naturales de Mendoza: Relatorio, I (13), pp. 161–172.

Bertotto, G.W., 2000. Cerro Agua Poca, un cono basáltico cuarternario portador de xenolithos ultramáficos, en el oeste de la provincia de la Pampa, Argentina. Revista de la Asociación Geológica Argentina 55 (1/2), 59–71.

Bertotto, G.W., 2003. Evolución geológica y petrológica de los conos basálticos cenozoicos portadores de xenolithos ultramáficos del margen oriental de la provincia basáltica Andino-Cuyana, provincias de La Pampa y Mendoza. Unpublished PhD Thesis, 196 pp. Universidad Nacional de la Plata, La Plata.

Bertotto, G.W., Bjerg, E.A., Cingolani, C.A., 2006. Hawaiin and Strombolian style monogenetic volcanism in the extra-Andean domain of central-west Argentina. Journal of Volcanology and Geothermal Research 158, 430–444.

Bertotto, G.W., Cingolani, C.A., Bjerg, E.A., 2009. Geochemical variations in Cenozoic backarc basalts at the border of La Pampa and Mendoza provinces, Argentina. Journal of South American Earth Sciences 28, 360–373.

Bowen, N.L., 1922. The behaviour of inclusions in igneous magmas. Journal of Geology 30, 513–570.

Burd, A., Booker, J.R., Pomposiello, M.C., Favetto, A., Larsen, J., Giordanengo, G., Bernal, L.O., 2008. Electrical conductivity beneath the Payún Matrú Volcanic Field in the Andean backarc of Argentina near 36.5°S: insights into the magma source. 7th Int. Symp. And. Geod., Nice, ext. abstract, pp. 90–93.

Cahill, T.A., Isacks, B.L., 1992. Seismicity and shape of the subducted Nazca plate. Journal of Geophysical Research 97 (B12), 17,503–17,529.

Costa, C.H., Cisneros, H., Salvarredi, J., Gallucci, A., 2004. Nuevos datos y reconsideraciones sobre la neotectónica del margen oriental del bloque de San Rafael, 12° Reunión sobre Microtectónica y Geología Estructural (Cafayate). Resúmenes 7.

Costa, C.H., Cisneros, H., Salvarredi, J., Gallucci, A., 2006. La neotectónica del margen oriental del Bloque de San Rafael: Nuevas consideraciones. Asociación Geológica Argentina, Serie D, Publicacion Especial 6, 33–40.

Douglass, J., Schilling, J.-G., Fontignie, D., 1999. Plume–ridge interactions of the Discovery and Shona mantle plumes with the southern mid-Atlantic ridge (40–55°S). Journal of Geophysical Research 104 (B2), 2941–2962.

Dyhr, C.T., Holm, P.M., Llambías, E.J., Dyhr, C.T., Holm, P.M., Llambías, E.J., 2013a. Geochemical constraints on the relationship between the Miocene-Pliocene volcanism and tectonics in the Palaoco and Fortunoso volcanic fields, Mendoza Region, Argentina: new insights from $^{40}Ar/^{39}Ar$ dating, Sr-Nd-Pb isotopes and trace elements. in prep. a Journal of Volcanology and Geothermal Research (In review).

Dyhr, C.T., Holm, P.M., Llambías, E.J., Scherstén, A., 2013b. Subduction controls on Miocene back-arc lavas from Sierra de Huantraico and La Matancilla and new $^{40}Ar/^{39}Ar$ dating from the Mendoza region, Argentina. in prep. b Lithos (In review).

Españon, V.R., 2010. Cosmogenic ^{21}Ne and ^{3}He dating and geochemistry of young basaltic lavas from southern Mendoza, Argentina. Master thesis University of Wollongong.

Folguera, A., Bottesi, G., Zapata, T., Ramos, V.A., 2008. Crustal collapse in the Andean backarc since 2 Ma: Tromen volcanic plateau, Southern Central Andes (36°40′–37°30′S). Tectonophysics 459, 140–160.

Folguera, A., Naranjo, J.A., Orihashi, Y., Sumino, H., Nagao, K., Polanco, E., Ramos, V.A., 2009. Retroarc volcanism in the northern San Rafael block (34°–35°30′S), southern Central Andes: occurrence, age and tectonic setting. Journal of Volcanology and Geothermal Research 186, 169–185.

Fontignie, D., Schilling, J.-G., 1996. Mantle heterogeneities beneath the South Atlantic: a Nd–Sr–Pb isotope study along the mid-Atlantic ridge (3°S–46°S). Earth and Planetary Science Letters 142, 209–221.

Galland, O., Hallot, E., Cobbold, P.R., Ruffet, G., de Bremond d'Ars, J., 2007. Volcanism in a compressional Andean setting: a structural and geochronological study of Tromen volcano (Neuquen province, Argentina). Tectonics 26, TC4010. http://dx.doi.org/10.1029/2006TC002011.

Germa, A., Quidelleur, X., Gillot, P.Y., Tchilinguirian, P., 2010. Volcanic evolution of the backarc Pleistocene Payún Matrú volcanic field (Argentina). Journal of South American Earth Sciences 29, 717–730.

Ghiorso, M.S., Sack, R.O., 1995. Chemical mass-transfer in magmatic processes IV. A revised and internally consistent thermodynamic model for the interpolation and extrapolation of liquid–solid equilibria in magmatic systems at elevated temperatures and pressures. Contributions to Mineralogy and Petrology 119 (2–3), 197–212.

Giambiagi, L., Bechis, F., García, V., Clark, A.H., 2008. Temporal and spatial relationships of thick- and thin-skinned deformation: a case study from the Malargüe fold-and-thrust belt, southern Central Andes. Tectonophysics 459, 123–139.

Gilbert, H., Beck, S., Zandt, G., 2006. Lithospheric and upper mantle structure of central Chile and Argentina. Geophysical Journal International 165, 383–398.

Glazner, A.F., Lang Farmer, G., Hughes, W.T., Wooden, J.L., Pickthorn, W., 1991. Contamination of basaltic magma by mafic crust at Amboy and Pisgah craters, Mojave desert, California. Journal of Geophysical Research 96 (B8), 13,673–13,691.

González Díaz, E.F., 1972. Descriptión geológica de la Hoja 30d Payún-Matrú, Provincia de Mendoza. Dirección Nacional de Geología y Minería, Boletín, 130, pp. 1–88.

Gudnason, J., Holm, P.M., Søager, N., Llambías, E.J., 2012. Geochronology of the late Pliocene to recent volcanic activity in the Payenia back-arc volcanic province, Mendoza, Argentina. Journal of South American Earth Sciences 37, 191–201.

Guzmán, C., Cristallini, E., Bottesi, G., 2007. Contemporary stress orientations in the Andean retroarc between 34°S and 39°S from borehole breakout analysis. Tectonics 26.

Hanan, B.B., Kingsley, R.H., Schilling, J.-G., 1986. Pb isotope evidence in the South Atlantic for migrating ridge-hot spot interactions. Nature 322, 137–144.

Hernando, I.R., Llambías, E.J., González, P.D., Sato, K., 2012. Volcanic stratigraphy and evidence of magma mixing in the Quarternary Payun Matru volcano, andean backarc in western Argentina. Andean Geology 39 (1), 158–179.

Herzberg, C., Asimov, P.D., 2008. Petrology of some oceanic island basalts: PRIMELT2.XLS software for primary magma calculation. Geochemistry, Geophysics, Geosystems 9, 9. http://dx.doi.org/10.1029/2008GC002057.

Herzberg, C., Gazel, E., 2009. Petrological evidence for secular cooling in mantle plumes. Nature 458, 619–623.

Herzberg, C., Asimov, P.D., Arndt, N., Niu, Y., Lesher, C.M., Fitton, J.G., Cheadle, M.J., Saunders, A.D., 2007. Temperatures in ambient mantle and plumes: constraints from basalts, picrites, and komatiites. Geochemistry, Geophysics, Geosystems 8, 2. http://dx.doi.org/10.1029/2006GC001390.

Hildreth, W., Moorbath, S., 1988. Crustal contributions to arc magmatism in the Andes of central Chile. Contributions to Mineralogy and Petrology 98, 455–489.

Holm, P.M., Søager, N., Dyhr, C.T., 2013p. The role of crust and fluids in the generation of arc magmas in the SVZ of the Andes (in prep.).

Humphris, S.E., Thompson, G., Schilling, J.-G., Kingsley, R.H., 1985. Petrological and geochemical variations along the mid-Atlantic Ridge between 46°S and 32°S: influence of the Tristan da Cunha mantle plume. Geochimica et Cosmochimica Acta 49, 1445–1464.

Irvine, T.N., Barager, W.R.A., 1971. A guide to the chemical classification of the common rocks. Canadian Journal of Earth Sciences 8, 523–548.

Kay, S.M., 2001. Terciary to recent magmatism and tectonics of the Neuquén basin between 36.5° and 38°S latitude. Report to Repsol/YPF. (210 pp.).

Kay, S.M., 2002. Tertiary to recent transient shallow subduction zones in the Central and Southern Andes. Congr. Geol. Argentino, Calafate, 15, 3, pp. 282–283.

Kay, S.M., Copeland, P., 2006. Early to middle Miocene backarc magmas of the Neuquén basin: geochemical consequences of slab shallowing and the westward drift of South America. Geological Society of America, Special Paper 407, 185–213.

Kay, S.M., Jones, H., 2011. Geochemical clues to the origin of the Auca Mahuida volcanic field in the Payenia backarc province of northern Neuquén. Abstract, XVIII Congr. Geol. Argentino, Neuquèn, 2011.

Kay, S.M., Orrell, S., Abbruzzi, J.M., 1996. Zircon and whole rock Nd–Pb isotopic evidence for a Grenville age and a Laurentian origin for the Precordillera terrane in Argentina. Journal of Geology 104, 637–648.

Kay, S.M., Gorring, M., Ramos, V.A., 2004. Magmatic sources, setting, and causes of Eocene to Recent Patagonian plateau magmatism (36° S to 52° S latitude). Revista de la Asociación Geológica Argentina 59 (4), 556–568.

Kay, S.M., Godoy, E., Kurtz, A., 2005. Episodic arc migration, crustal thickening, subduction erosion, and magmatism in the south-central Andes. Geological Society of America Bulletin 117 (1–2), 67–88.

Kay, S.M., Burns, W.M., Copeland, P., Mancilla, O., 2006a. Upper Cretaceous to Holocene magmatism and evidence for transient Miocene shallowing of the Andean subduction zone under the northern Neuquén Basin. Geological Society of America, Special Paper 407, 19–60.

Kay, S.M., Copeland, P., Mancilla, O., 2006b. Evolution of the late Miocene Chachahuén volcanic complex at 37 °S over a transient shallow subduction zone under the Neuquén Andes. Geological Society of America, Special Paper 407, 215–246.

Kay, S.M., Ardolino, A.A., Gorring, M.L., Ramos, V.A., 2007. The Somuncura large igneous province in Patagonia: interaction of a mantle thermal anomaly with a subducting slab. Journal of Petrology 48 (1), 43–77.

Kendrick, E., Bevis, M., Smalley Jr., R., Brooks, B., Vargas, R.B., Lauria, E., Souto, L.P., 2003. The Nazca-South America Euler vector and its rate of change. Journal of South American Earth Sciences 16, 125–131.

Kennedy, A.K., Lofgren, G.E., Wasserburg, G.J., 1993. An experimental study of trace element partitioning between olivine, orthopyroxene and melt in chondrules — equilibrium values and kinetic effects. Earth and Planetary Science Letters 115, 177–195.

Klotz, J., Khazaradze, G., Angermann, D., Reigber, C., Perdomo, R., Cifuentes, O., 2001. Earthquake cycle dominates contemporary crustal deformation in Central and Southern Andes. Earth and Planetary Science Letters 193, 437–446.

Kogiso, T., Hirschmann, M.M., Pertermann, M., 2004. High-pressure partial melting of mafic lithologies in the mantle. Journal of Petrology 45 (12), 2407–2422.

Kystol, J., Larsen, L.M., 1999. Analytical procedures in the Rock Geochemical Laboratory of the Geological Survey of Denmark and Greenland. Geology of Greenland Survey Bulletin 184, 59–62.

Lauritsen, S.N., 2010. Klinopyroxen-barometri af magmaer fra Payenia og en petrologisk undersøgelse af udviklede bjergarter fra Palauco, Mendoza (Master thesis, unpublished).

Le Maître, R.W., Streckeisen, A., Zanettin, B., Le Bas, M.J., Bonin, B., Bateman, P., Bellieni, G., Dudek, A., Efremova, S., Keller, J., Lameyre, J., Sabine, P.A., Schmid, R., Sorensen, H., Woolley, A.R. (Eds.), 2002. Igneous Rocks; A Classification and Glossary of Terms; Recommendations of the International Union of Geological Sciences Subcommission on the Systematics of Igneous Rocks, 2nd ed. Cambridge University Press, Cambridge, United Kingdom, p. 236.

Le Roux, P.J., 2000. The geochemistry of selected mid-ocean ridge basalts from the southern mid-Atlantic ridge (40–55°S). PhD thesis University of Cape Town.

Le Roux, P.J., le Roex, A.P., Schilling, J.-G., Shimizu, N., Perkins, W.W., Pearce, N.J.G., 2001. Mantle heterogeneity beneath the southern mid-Atlantic ridge: trace element evidence for contamination of ambient asthenospheric mantle. Earth and Planetary Science Letters 203, 479–498.

Le Roux, P.J., le Roex, A.P., Schilling, J.-G., 2002. Morb melting processes beneath the southern mid-Atlantic ridge (40–55°S): a role for pyroxenite and residual garnet. Contributions to Mineralogy and Petrology 144, 206–229.

Litvak, V.D., Folguera, A., Ramos, V.A., 2008. Determination of an arc-related signature in late Miocene volcanic rocks over the San Rafael block, Southern Central Andes (34°30′–37°S), Argentina: the Payenia shallow subduction zone. 7th Int. Symp. And. Geodyn., Nice, ext. abstracts, pp. 289–291.

Llambías, E.J., 1966. Geología y petrografía del volcán Payún-Matrú. Acta Geologica Lilloana 8, 265–310.

Llambías, E.J., Kleiman, L.E., Salvarredi, J.A., 1993. El magmatismo Gondwánico. 12° Congreso Geológico Argentino y 2° Congreso de Exploración de Hidrocarburos (Mendoza). In: Ramos, V.A. (Ed.), Geología y Recursos Naturales de Mendoza: Relatorio, I (6), pp. 53–64.

Llambías, E.J., Bertotto, G.W., Risso, C., Hernando, I., 2010. El volcanismo Cuarternario en el retroarco de Payenia: una revision. Revista de la Asociación Geológica Argentina 67 (2), 278–300.

Manacorda, L., Reinante, S.M.E., Cazau, L., Penna, E., 2002. Los reservorios del Grupo Neuquén. In: Schiuma, M., Hinterwimer, G., Vergani, G. (Eds.), Rocas Reservorio de las Cuencas Productivas de la Argentina: 5° Congr. Expl. Desarrollo Hidrocarb., Mar del Plata, pp. 529–550.

Mazzarini, F., Fornaciai, A., Bistacchi, A., Pasquarè, F.A., 2008. Fissural volcanism, polygenetic volcanic fields, and crustal thickness in the Payen Volcanic Complex on the central Andes foreland (Mendoza, Argentina). Geochemistry, Geophysics, Geosystems 9, 9.

McDonough, W.F., Sun, S.-S., 1995. Composition of the earth. Chemical Geology 120, 223–253.

McKenzie, D., Bickle, M.J., 1988. The volume and composition of melt generated by extension of the lithosphere. Journal of Petrology 29, 625–679.

McKenzie, D., O'Nions, R.K., 1995. The source region of ocean island basalts. Journal of Petrology 36, 133–159.

Melchor, R., Casadío, S., 1999. Hoja geológica 3766-III La Reforma, provincia de la Pampa. Secretaría de Minería de la Nación. SEGEMAR, Boletín, 295. Secretaria de Mineria de la Nacion in Argentina, Buenos Aires (63 pp.).

Middlemost, E.A.K., 1989. Iron oxidation ratios, norms and the classification of volcanic rocks. Chemical Geology 77, 19–26.

Muñoz Bravo, J., Stern, C.R., Bermudez, A., Delpino, D., Dobbs, M.F., Frey, F., 1989. El volcanismo Plio-Cuaternario a traves de los 34–39°S de los Andes. Revista de la Asociación Geológica Argentina XLIV (1–4), 270–286.

Nullo, F.E., Stephens, G.C., Otamendi, J., Baldauf, P.E., 2002. El volcanismo del Terciario superior del sur de Mendoza. Revista de la Asociación Geológica Argentina 57 (2), 119–132.

Núñez, E., 1976. Descripción geológica de la Hoja 31e Chical-Có, provincias de Mendoza y La Pampa. Servicio Nacional Geológico Minero, Informe Inédito.Servicio Nacional Geologico Minero in Argentina.

Ostera, H., Dapeña, C., 2003. Environmental isotopes and geochemistry of Bañado Carilauquen, Mendoza, Argentina. 4° S. Amer. Sym. Isot. Geol., Salvador, pp. 461–464.

Pasquaré, G., Bistacchi, A., Mottana, A., 2005. Gigantic individual lava flows in the Andean foothills near Malargüe (Mendoza, Argentina). Rendiconti Fisici dell'Accademia dei Lincei 9 (16), 127–135.

Pasquarè, G., Bistacchi, A., Francalanci, L., Bertotto, G.W., Boari, E., Massironi, M., Rossotti, A., 2008. Very long pahoehoe inflated basaltic lava flows in the Payenia volcanic province (Mendoza and La Pampa, Argentina). Revista de la Asociación Geológica Argentina 63 (1), 131–149.

Philpotts, J.A., Schnetzler, C.C., 1970. Phenocrysts-matrix partition coefficients for K, Rb, Sr and Ba, with applications to anorthosite and basalt genesis. Geochimica et Cosmochimica Acta 34 (3), 307–322.

Ramos, V.A., 2004. Cuyania, an exotic block to Gondwana: review of a historical success and the present problems. Gondwana Research 7 (4), 1009–1026.

Ramos, V.A., Folguera, A., 2011. Payenia volcanic province in the Southern Andes: an appraisal of an exceptional Quaternary tectonic setting. Journal of Volcanology and Geothermal Research 201 (1–4), 53–64.

Ramos, V.A., Kay, S.M., 2006. Overview of the tectonic evolution of the southern Central Andes of Mendoza and Neuquén (35–39°S latitude). Geological Society of America, Special Paper 407, 1–17.

Reiners, P.W., Nelson, B.K., Ghiorso, M.S., 1995. Assimilation of felsic crust by basaltic magma: thermal limits and extents of crustal contamination of mantle-derived magmas. Geology 23 (6), 563–566.

Risso, C., Németh, K., Combina, A.M., Nullo, F., Drosina, M., 2008. The role of phreatomagmatism in a Plio-Pleistocene high-density scoria cone field: Llancanelo Volcanic Field (Mendoza), Argentina. Journal of Volcanology and Geothermal Research 169, 61–86.

Rudnick, R.L., Gao, S., 2003. Composition of the continental crust. In: Holland, H.D., Turekian, K.K. (Eds.), Treatise on Geochemistry: The crust, pp. 1–64.

Shaw, D.M., 1970. Trace element fractionation during anatexis. Geochimica et Cosmochimica Acta 34, 237–243.

Smith, P.M., Asimow, P.D., 2005. Adiabat_1ph: a new public front-end to the MELTS, MELTS, and pHMELTS models. Geochemistry, Geophysics, Geosystems 6, 1.

Stern, C.R., 1991. Role of subduction erosion in the generation of the Andean magmas. Geology 19, 78–81.

Stern, C.R., 2011. Subduction erosion: rates, mechanisms, and its role in arc magmatism and the evolution of the continental crust and mantle. Gondwana Research 20, 284–308.

Stern, C.R., Skewes, M.A., 1995. Miocene to Present magmatic evolution at the northern end of the Andean Southern Volcanic Zone, Central Chile. Revista Geologica de Chile 22, 261–272.

Stern, C.R., Frey, F.A., Futa, K., Zartman, R.E., Peng, Z., Kyser, K.T., 1990. Trace element and Sr, Nd, Pb, and O isotopic composition of Pliocene and Quaternary alkali basalts of the Patagonian Plateau lavas of southernmost South America. Contributions to Mineralogy and Petrology 104, 294–308.

Stern, C.R., Moreno, H., López-Escobar, L., Clavero, J.E., Lara, L.E., Naranjo, J.A., Parada, M.A., Skewes, M.A., 2007. Chilean volcanoes. In: Moreno, T., Gibbons, W. (Eds.), The Geology of Chile. Geol. Soc. Lond. Press, pp. 149–180 (chapter 5).

Stern, C.R., Floody, R., Espiñeíra, D., 2011. Olivine–hornblende–lamprophyre dikes from Quebrada los Sapos, El Teniente, Central Chile (34°S): implications for the temporal geochemical evolution of the Andean subarc mantle. Andean Geology 38 (1), 1–22.

Stracke, A., Bourdon, B., 2009. The importance of melt extraction for tracing mantle heterogeneity. Geochimica et Cosmochimica Acta 73, 218–238.

Tassara, A., Götze, H.-J., Schmidt, S., Hackney, R., 2006. Three-dimensional density model of the Nazca plate and the Andean continental margin. Journal of Geophysical Research 111, B9.

Turcotte, D.L., Schubert, G., 2002. Geodynamics. Cambridge University Press (456 pp.).

Turienzo, M., 2010. Structural style of the Malargüe fold-and-thrust belt at the Diamante River area (34°30′–34°50′S) and its linkage with the Cordillera Frontal, Andes of central Argentina. Journal of South American Earth Sciences 29, 537–556.

Varekamp, J.C., Maarten deMoor, J., Merrill, M.D., Colvin, A.S., Goss, A.R., Vroon, P.Z., Hilton, D.R., 2006. Geochemistry and isotopic characteristics of the Caviahue–Copahue volcanic complex, Province of Neuquén, Argentina. Geological Society of America, Special Paper 407, 317–342.

Varekamp, J.C., Hesse, A., Mandeville, C.W., 2010. Back-arc basalts from the Loncopue graben (Province of Neuquén, Argentina). Journal of Volcanology and Geothermal Research 197 (1–4), 313–328.

Wang, K., Hu, Y., Bevis, M., Kendrick, E., Smalley Jr., R., Vargas, R.B., Lauria, E., 2007. Crustal motion in the zone of the 1960 Chile earthquake: detailing earthquake-

cycle deformation and forearc-sliver translation. Geochemistry, Geophysics, Geosystems 8, Q10010. http://dx.doi.org/10.1029/2007GC001721.
Willbold, M., Stracke, A., 2006. Trace element composition of mantle end-members: implications for recycling of oceanic and upper and lower continental crust. Geochemistry, Geophysics, Geosystems 7, 4. http://dx.doi.org/10.1029/2005GC001005.
Yrigoyen, M.R., 1993. Los depositos sinorogenicos Terciarios. In: Ramos, V.A. (Ed.), XII° Congr. Geol. Argentino and II° Cong. Explor. Hidrocarb. (Mendoza 1993), Geol. Recur. Nat. Mendoza: Relatorio, 1, 11, pp. 123–148.
Zindler, A., Hart, S.R., 1986. Chemical geodynamics. Annual Review of Earth and Planetary Sciences 14, 493–571.